IEEE Access
Multidisciplinary | Rapid Review | Open Access Journal

Received September 14, 2021, accepted October 24, 2021, date of publication November 2, 2021,
date of current version November 23, 2021.

Digital Object Identifier 10.1109/ACCESS.2021.3125135

AI-Based Approach for Optimal Placement of EVCS and DG With Reliability Analysis

MOHD BILAL[1], M. RIZWAN[1], (Senior Member, IEEE), IBRAHIM ALSAIDAN[2], (Member, IEEE), AND FAHAD M. ALMASOUDI[3], (Member, IEEE)

[1]Department of Electrical Engineering, Delhi Technological University, Delhi 110042, India
[2]Department of Electrical Engineering, College of Engineering, Qassim University, Buraydah, Qassim 52571, Saudi Arabia
[3]Department of Electrical Engineering, Faculty of Engineering, University of Tabuk, Tabuk 47913, Saudi Arabia

Corresponding author: Mohd Bilal (bilal.zhcet01@gmail.com)

The authors would like to thank the Chair of Prince Faisal for Artificial intelligence research (CPFAI) for funding this research work through the project number QU-CPFAI-2-9-5. Also would like to extend their appreciation to the Deputyship for Research & Innovation, Ministry of Education and the Deanship of Scientific Research, Qassim University for their support for this research.

ABSTRACT It is expected that future transport will rely on electric vehicles (EVs) due to their sustainability and reduced greenhouse gas emissions. However, the rapid increase in electric load penetration causes several other concerns, including a generation-demand mismatch, increased network active power loss, a degradation in voltage profile, and decreased voltage stability margin. To overcome the issues mentioned earlier, proper integration of electric vehicle charging stations (EVCS) at appropriate locations is essential. The connection of an EVCS to the electricity grid will bring new challenges. Distributed generation (DG) sources are incorporated with EVCS to lessen the impact of EV charging load. In this study, charging stations are combined with DG units, which increases the motivation to use EVs. This study proposes an artificial intelligence (AI) approach, the hybrid of grey wolf optimization and particle swarm optimization, i.e., HGWOPSO, to investigate the suitable nodes for EVCS and DGs in a balanced distribution system. The proposed methodology is verified on the IEEE-33 bus and IEEE-69 bus systems. According to the findings, the obtained results are consistent as compared to other existing techniques. These findings are taken into consideration to analyze the reliability of electrical distribution networks. It is stated that using adequate reliability data of appropriately integrated DG and EVs increases the electrical system's reliability.

INDEX TERMS Artificial intelligence, electric vehicle, charging stations, radial distribution system, distributed generators, reliability.

I. INTRODUCTION

The substantial increase in temperature and ample release of carbon footprint due to the excessive usage of conventional vehicles impose a detrimental effect on the ecology. Global warming harms the ecological system of the earth due to the non-uniform rains and temperature rise. So, an electrified form of transportation, i.e., battery-based transport, is the need of the hour to overcome the pollution effects caused by the traditional mode of transportation [1]. The advent of electric vehicles (EVs) and their increasing development have many benefits, including saving on fossil fuels and reducing air pollution. Many countries around the globe are adopting the battery-based mode of transportation for the sake of pollution minimization. Due to this concern, EVs have reached 28.8% in Norway, 6.5% in Netherland, and 1.5% in China. In addition to this, various countries are planning to employ 100 % EVs as a future transportation mode. It is expected that almost 35 million EVs will run globally by the end of 2022. Apart from the fact that EVs are environmentally beneficial, their charging has the potential to have a profound influence on the electrical power system's reliability. Due to the increment in system load caused by EV charging, the substation reserve capacity and feeder load transfer capabilities are reduced. During system renovation utilizing other feeders, the ability of load transfer is also essential. This has an immediate effect on the system's reliability [2]. Furthermore, if EVs are charged using traditional power sources, the goal

The associate editor coordinating the review of this manuscript and approving it for publication was Christopher H. T. Lee.

of EV utilization is not accomplished. On the other hand, the utilization of solar/wind energy for charging the EV load, maximizes the merits of EVs.

EVs are originally connected to the grid to charge their batteries. On the other hand, new smart grid technologies enable increased opportunities in energy transfer to the grid and are referred to as the vehicle-to-grid (V2G) mode. EVs that are associated with the power network serve as energy storage devices [3].

In accordance with electricity directives planned by European Union, the distribution system operators (DSOs) are accountable for giving amenities to associated customers and distributed generations (DGs) as well as delivering network modifications for EV charging stations (EVCS) [4]. The charging locations and periods are outside the control of DSOs. As a result of the variability in EV charging, system operation turns out to be serious. A recent study on the influence of EV integration on generation systems has shown some interesting results [5]. The focus of reference [6] is on the impact of EV charging on the power generation system and CO_2 emissions reduction. The influence of EVs on emissions produced from electricity generation and transportation sectors is investigated in a fictional way.

The influence of EVs on electrical distribution systems is examined using various EV scenarios and charging management methodologies [7]. The influence of charging procedures on the load profile is described [8]. Various penetration levels of EVs to evaluate the influence of EVs on system power losses are investigated [9]. The impact of EV charging on distribution transformer aging in the presence of rooftop solar photovoltaic systems was studied by the authors in [10]. The influence of charging on low-voltage residential distribution systems using a case study for the year 2030 is examined [11]. The integration of EVCS into the distribution system increases the overall load of the network. The influence of erecting the EVCS in a distribution network can be analyzed by properly modeling EVCS in a distribution system [12]. A qualitative study has been attempted for the optimal planning of EVCS based on the transportation system, distribution system, and coupled transportation-distribution system [13]. The reliability analysis of the distribution network after integrating the EVCS has been described [14]. The author presents the scheduling strategy of EVCS and provides an insight into how the reliability can be improved and reduce the negative effect on the power network [15]. The optimum placement of EVCS in the IEEE-33 bus radial network has been discussed, considering uncertainties related to the quantity of EVs to be charged [16]. GWO/WOA has been employed to tackle the aforesaid issues. The EVCS planning in distribution network superimposed with road network have been performed. Uncertainties related to EVs are considered using the 2m Point Estimation Method. Differential evolution and Harris Hawks Optimization algorithm have been utilized for optimizing the objectives [17]. Optimal placement of EVCS has been performed in the Beijing district with the aim of minimizing the total cost and power loss [18]. A hybrid approach of chicken swarm optimization and teaching learning-based optimization is used for EVCS allocation considering various economic and grid operating issues [19]. Authors in [20] present a comprehensive methodology for effectively placing solar-based EVCS in a distribution network with enhanced voltage profile, minimal power loss, and lower cost. A stochastic technique is employed to anticipate projected EV load demand at EVCS, and a Feed-forward neural network is used to analyze estimated solar power from the attached PV plant in the suggested methodology. Different charging procedures were discussed and their impact on daily peak loads was examined [21]. The incremental investments for various EV penetration levels, as well as energy losses, were computed by the authors in [22]. The influence of EV on distribution system reliability in addition to the negative effects on voltage and power losses is focused [23]. The impact of electric motor vehicles on grid reliability is studied in [24].

Some research works are concentrated on mitigating the severity of EVs on the power system. In [25], the authors present a sustainable, intelligent load balancing control approach for lowering electrical losses and improving system voltage. Reactive power regulation is utilized in EVCS to enhance the voltage profile [26]. The reliability and techno-economic benefits of DG integration have been demonstrated [27]. Therefore, DGs integration has been proposed as a viable approach for mitigating the charging consequences of EVs [28]. The author utilized particle swarm optimization for the EVCS and DGs allocation in an unbalanced radial distribution network [29]. The author suggested a hybrid grey wolf optimizer for 33-bus, 69-bus, and Indian 85-bus distribution networks to reduce power loss [30]. Authors have optimally allocated EVCS and DGs in 30 nodes and 69 nodes radial DS [31]. Genetic algorithm-based DG placement is performed considering IEEE-16 bus, IEEE-37 bus, and IEEE-75 bus radial DS as a test system [32].

Furthermore, the DG allocation problem in the IEEE-33 bus radial distribution system using particle swarm optimization is presented [33]. However, a hybrid of genetic algorithm and particle swarm optimization is proposed to reduce power loss and improve voltage profile and stability for optimal DGs allocation [34]. The impact of renewable-based DGs on IEEE distribution grids with 33 and 69 nodes, as well as one of Egypt's radial distribution networks as a practical network, is examined within 24 hours at different loading conditions [35]. Authors in [36] created optimization models to collectively manage the locations and sizes of EVCS, solar photovoltaic power plants, and energy storage systems in power systems while considering future power strategic management. The author employed modified single and multi-objective Harris Hawks Optimization algorithms for obtaining the nodes to optimally locate the DGs in the radial power network. Finding ideal nodes is done with the goals of minimizing power loss, preserving voltage levels, and improving the voltage stability index [37]. The authors of [38] proposed an indicator for determining the best

location for DGs in electrical networks. This indicator is used to address a variety of issues, such as total electrical loss minimization, energy not supplied, and voltage variation. By system reconfiguration and the integration of solar/wind-based DGs, another endpoint, namely annual energy reduction loss, is seen [39]. Additionally, an innovative two-stage stochastic programming method is presented, and the uncertainty issues, as well as load fluctuation, are investigated, particularly for wind and solar energy production [40]. The overall cost is decreased in this technique by including battery storage systems into the distribution network and planning for demand response programs. Simultaneously, due to the appropriate size of battery energy storage and optimal position, the improved reliability of power system reliability is obtained. A multi-objective optimization model is presented with the objective of reducing power loss, improving voltage deviation, and cost in order to assign EVCS and capacitors in candidate buses optimally [41]. In an unbalanced distribution system, solar PV units are used to adjust for EV charging demand [42]. Cost, dependability, power losses, and voltage profile are all taken into account when synchronizing charging stations and DGs [43]. Capacity reinforcement with DGs is recommended to offset the growing penetration of EVs, with reliability improvement as one of the objectives [44]. The authors in [45] discuss the development of a charging station that incorporates wind production and storage. The best DG penetration level for a specific EV energy consumption is evaluated [46].

In the vision of the above, the majority of related literature and studies are focused on the impact of EVs on voltage level and system losses, with little emphasis on reliability. EVs are another category of load that enters the grid network, and the reliability of these EV loads is largely overlooked. Despite the abundance of research on DG siting and sizing in the literature, its impact on the reliability of grid networks is a growing subject of research that has received little attention in previous studies. Furthermore, the majority of the prior meta-heuristic optimization algorithm-related methods presented are complicated in construction, entail a large set of network parameters, and trap in local optimal solutions. Additionally, several types of research used a very rigorous statistical framework that required a lot of information based on descriptive approaches. Unlike analytical processes, metaheuristic methods are easy to adopt, take less time, have fewer parameters to manage, and can produce relevant results. The suggested hybrid technique eliminates these shortcomings while remaining simple to execute and achieving good convergence. Therefore, the use of a hybrid intelligent methodology for DGs allocation in the presence of EVCS in a radial distribution network will be demonstrated in this work. Hybrid algorithms integrate the best features of both algorithms to provide superior results.

Inspired by the existing research in the optimal allocation of EVCS, a hybrid optimization strategy is suggested for the optimal planning of EVCS. DGs units are utilized to reduce the charging impact of EVs. DGs are used in the suggested technique to preserve voltage profile, reduce active power loss and improve reliability. The integration of EVCS and DGs to the system adds extra demand to the system, affecting the power loss. The joint impact of EVs and DG integration is considered for two standard test systems. The efficacy of the suggested method is tested in MATLAB, and the results are equated with present techniques. The fundamental system reliability indicators, such as the system average interruption frequency index (SAIFI), system average interruption duration index (SAIDI), Customer Average Interruption Duration Index (CAIDI), and expected energy not supplied (EENS) and average energy not supplied (AENS), etc., are used to examine the impact on system reliability.

Finally, the contribution of the proposed work is summarized as follows:

- The calculation of objective functions is done using a faster and effective direct search-based load flow method.
- The influence of EV penetration on the reliability of the distribution system is investigated.
- Multiple DG units are appropriately introduced into the distribution system to reduce the active power losses, strengthening the voltage profile and enhancing the voltage stability index.
- Integration of DG units with charging stations to enhance the reliability of distribution network.
- To demonstrate the efficiency and performance of the proposed HGWOPSO, standard test networks, i.e., 33-bus and 69-bus systems are considered.
- The simulation results achieved with the suggested hybrid method are compared to those obtained with other methods.

The work will continue to be done in order to complete the contributions as follows: Mathematical formulation of the problem and objective functions is given in section II. Section III formulates and explains the basic concepts of reliability parameters. The proposed optimization methodology is presented in section IV. Essential findings and discussions are contained in section V. Concluding remarks are given in section VI.

II. MATHEMATICAL FORMULATION OF PROBLEM

In general, load fluctuates with time at the distribution side in the electrical power network; however, the best site and size of EVCS and DG allocation with fluctuating load is not acceptable. Hence, the following assumptions are applied to the problem of optimal DG and EVCS allocation planning [47].

1) Radial distributions systems are balanced in nature.
2) Constant capacities EVCS are employed.
3) DGs having power factor unity are used in radial DS.
4) The DGs output is not time-varying.
5) The load has constant active and reactive power.

DGs are represented as negative loads in this work because they do not modulate the bus voltage. The best location and capacity of DG should be attained without violating the

system constraint, which must be validated at every iteration using load flow analysis. Active power losses, voltage profile improvement, and voltage stability enhancement are basic objective functions that are investigated.

A. DIRECT APPROACH METHOD FOR POWER FLOW

The majority of distribution networks are radial in construction and have a low reactance to resistance ratio. Conventional load flow-based technique such as Gauss-Seidel and Newton Raphson is ineffective. Hence, power flow is performed in this article utilizing a direct search-based load flow approach [48].

The proposed power flow method relies on forming two matrices, such as bus injection to branch current (BIBC) and branch current to bus voltage (BCBV). Simple multiplication of these two matrices is done to find load flow solutions. A simple 6-bus distribution network is depicted in Fig. 1., where $P_1 - P_5$ represents the branch currents and $Z_{12} - Z_{56}$ are the impedance of respective branches.

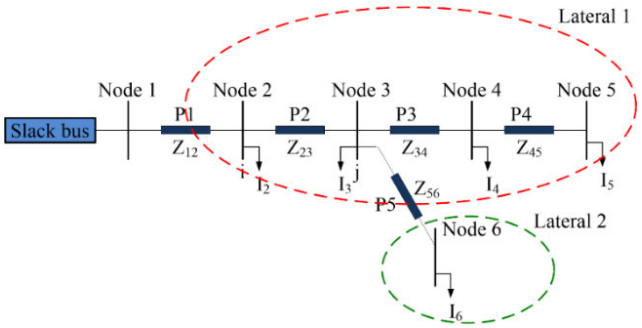

FIGURE 1. A simple 6-bus distribution network.

The current injected at node i can be calculated as

$$I_i = \left(\frac{P_i + jQ_i}{V_i}\right)^* \tag{1}$$

where, I_i, P_i, Q_i and V_i denotes the current, real power, reactive power, and voltage at i^{th} bus respectively.

The current in Eq. (1) can be further disintegrated to its active and reactive parts.

$$Real\ (I_i) = \frac{P_i cos\theta_i + Q_i sin\theta_i}{|V_i|} \tag{2}$$

$$Imag\ (I_i) = \frac{P_i sin\theta_i - Q_i cos\theta_i}{|V_i|} \tag{3}$$

where, θ_i designate the voltage angle at i^{th} bus.

B is the branch current matrix as illustrated in Fig. 1, and matrix P is calculated using Kirchhoff's current law (KCL) with the help of Eq. (3).

$$\begin{bmatrix} P_1 \\ P_2 \\ P_3 \\ P_4 \\ P_5 \end{bmatrix} = \begin{bmatrix} 1 & 1 & 1 & 1 & 1 \\ 0 & 1 & 1 & 1 & 1 \\ 0 & 0 & 1 & 1 & 0 \\ 0 & 0 & 0 & 1 & 0 \\ 0 & 0 & 0 & 0 & 1 \end{bmatrix} \begin{bmatrix} I_1 \\ I_2 \\ I_3 \\ I_4 \\ I_5 \end{bmatrix} \tag{4}$$

$$[P] = [BIBC]\,[I] \tag{5}$$

On the other hand, the voltage drops at each bus in relation to the reference bus is computed using Kirchhoff's voltage law (KVL) as follows:

$$\begin{bmatrix} V_1 \\ V_1 \\ V_1 \\ V_1 \\ V_1 \end{bmatrix} - \begin{bmatrix} V_2 \\ V_3 \\ V_4 \\ V_5 \\ V_6 \end{bmatrix} = \begin{bmatrix} Z_{12} & 0 & 0 & 0 & 0 \\ Z_{12} & Z_{23} & 0 & 0 & 0 \\ Z_{12} & Z_{23} & Z_{34} & 0 & 0 \\ Z_{12} & Z_{23} & Z_{34} & Z_{45} & 0 \\ Z_{12} & Z_{23} & 0 & 0 & Z_{36} \end{bmatrix} \begin{bmatrix} P_1 \\ P_2 \\ P_3 \\ P_4 \\ P_5 \end{bmatrix} \tag{6}$$

$$[\Delta V] = [BCBV]\,[P] \tag{7}$$

Inserting the value of matrix P from Eq. (4) to Eq. (6), we get:

$$\begin{bmatrix} V_1 \\ V_1 \\ V_1 \\ V_1 \\ V_1 \end{bmatrix} - \begin{bmatrix} V_2 \\ V_3 \\ V_4 \\ V_5 \\ V_6 \end{bmatrix} = \begin{bmatrix} Z_{12} & 0 & 0 & 0 & 0 \\ Z_{12} & Z_{23} & 0 & 0 & 0 \\ Z_{12} & Z_{23} & Z_{34} & 0 & 0 \\ Z_{12} & Z_{23} & Z_{34} & Z_{45} & 0 \\ Z_{12} & Z_{23} & 0 & 0 & Z_{36} \end{bmatrix} * \begin{bmatrix} 1 & 1 & 1 & 1 & 1 \\ 0 & 1 & 1 & 1 & 1 \\ 0 & 0 & 1 & 1 & 0 \\ 0 & 0 & 0 & 1 & 0 \\ 0 & 0 & 0 & 0 & 1 \end{bmatrix} * \begin{bmatrix} I_1 \\ I_2 \\ I_3 \\ I_4 \\ I_5 \end{bmatrix} \tag{8}$$

$$[\Delta V] = [BCBV]\,[BIBC]\,[I] \tag{9}$$

$$[\Delta V] = [DLF]\,[I] \tag{10}$$

where DLF stands for distribution load flow matrix, which is used to determine voltage drop at each bus in relation to the reference bus. The following two steps are used to determine DLF.

Step 1: set branch impedance vector Z_b from the branch data.

Step 2: convert branch impedance vector to a diagonal matrix, with all upper and lower elements save to zero sets to zero except the element in the main diagonal positions and multiply the resulting matrix with I to obtain ΔV.

B. MULTI-OBJECTIVE FUNCTIONS

The principal target of this research work is to find out the optimum nodes for EVCS and DGs placement in the radial distribution system for lessening the active power losses of the network, monitoring the voltage profile within required limits, and enhancing voltage stability index (VSI), keeping in view that, all the subjected constraints must not be violated. EVCS supplies current for charging EVs. The EV battery capacity is defined in kilowatt-hour (kWh) and ampere-hour (Ah). The EVCS is modeled in such a way that it delivers only real current for EV charging [29]. When EVCS is placed at any bus of the distribution network causes an increment in real power only. Hence, it necessitates the placement of EVCS at that node (bus) where the minimum branch current flows. Regarding this, Fig. 2. shows a portion of the distribution network in which EVCS is located at $(k+1)^{th}$ bus and available connected load at the same bus takes

power from the grid.

$$\begin{aligned} &\min\left(F_1\left(x\right), F_2\left(x\right), F_3\left(x\right)\right) x \in \copyright \\ &subjected\ to\ g_u\left(x\right) = 0\ u = 1, 2, 3 \ldots., t \\ &\qquad h_v\left(x\right) = 0\ v = 1, 2, 3 \ldots., s \\ &\qquad x_L \leq x \leq x_U \end{aligned} \tag{11}$$

where, $g_u(x)$ are the equality constraint, $h_v(x)$ are the inequality constraint, t and s are the numbers of equality and inequality constraints, x_L and x_U are the lower bound and upper bound of variables, $\copyright$ is the variable space.

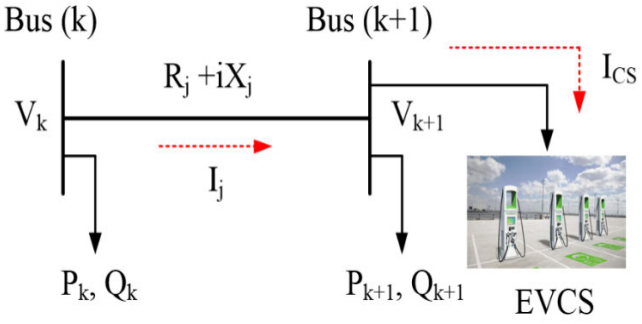

FIGURE 2. EVCS located at the bus of radial distribution system.

1) ACTIVE POWER LOSS (APL)

The largest power loss in an electric network typically occurs over the distribution system, which impacts annual sales. Consequently, the APL minimization is the major concern while allocating EVCS and DGs in radial distribution networks. The load flow analysis of the distribution network is conducted to determine the APL, i.e., base case power loss. The direct approach-based load flow analysis is performed in this article [48]. The active power loss after the load flow is determined using Eq. (12), and it depends on the amount of current drawn/injected into the bus [49].

$$APL = \sum_{i=1}^{N_{br}} |P_i|^2 * R_i = TPS(R) * |BIBC * I|^2 \tag{12}$$

where, P_i is the current flowing in i^{th} branch, R_i is the resistance of i^{th} branch, R is the branch resistance matrix, which contains all of the branches' resistances.

Because EVCS functions as a high load, it increases APL when it is deployed at any node in the distribution system. Therefore, the goal is to choose the bus that increases APL to the minimum. The additional losses of the distribution system can be offset by arranging the DGs optimally. The primary function of DG is to inject real and reactive power into the network, compensating for the losses caused by EVCS deployment.

When current I is disintegrated into its real and imaginary parts, Eq. (12) becomes as given below:

$$APL = \text{TPS (R)} * \left[\left(\text{BIBC} * \text{Real (I)}\right)^2 + \left(\text{BIBC} * \text{Imag (I)}\right)^2\right] \tag{13}$$

By putting the real and imaginary parts of current from Eq. (2) and Eq. (3) respectively to Eq. (13), the overall real power loss can be given as:

$$\min \text{F}_1 = \text{TPS (R)} * \left(\text{BIBC} * \frac{\text{Psin}\theta + \text{Qcos}\theta}{|\text{V}|}\right)^2 + \text{TPS (R)} * \left(\text{BIBC} * \frac{\text{Pcos}\theta + \text{Qsin}\theta}{|\text{V}|}\right)^2 \tag{14}$$

2) VOLTAGE DEVIATION INDEX (VDI)

The voltage quality of the bus is measured in terms of the voltage deviation index. As a result, bus VDI must be minimized in order to produce a more controlled bus voltage profile over the radial distribution network. Bus VDI is used as an objective function in the proposed optimal EVCS and DG allocation and is expressed as [50]:

$$\min \text{F}_2 = \sum_{\text{k=1}}^{\text{N}_{\text{bus}}} (\text{V}_\text{k} \text{V}_{\text{ref}})^2 \tag{15}$$

Each bus's voltage magnitude must lie between the minimum value (0.95 p.u) and maximum value (1.05 p.u).

3) VOLTAGE STABILITY INDEX (VSI)

In light of the voltage deviation alone, the distribution system's security level is insufficient. As a result, VSI is suggested as one of the main functions in this effort for enhanced voltage profiles. The distribution system's maximum VSI indicates that the bus can maintain its voltage profile within acceptable limits under varying loading conditions. The utility strives to keep the VSI of the distribution system near-unity of all buses for the safe operation of the system. VSI of distribution system can be formulated as follows:

$$VSI_{k+1} = |V_k|^4 - 4 * \left[P_{k+1}X_j - Q_{k+1}R_j\right]^2 - 4 * \left[P_{k+1}R_j - Q_{k+1}X_j\right]|V_k|^2 \tag{16}$$

where, $\text{VSI}_{\text{k+1}}$ represents the VSI of $(k+1)^{th}$ bus, R_j and X_j represents the resistance and reactance of j^{th} branch connecting the k^{th} and $(k+1)^{th}$ bus, $\text{P}_{\text{k+1}}$ denotes the active power at $(k+1)^{th}$ bus and $\text{Q}_{\text{k+1}}$ indicates the reactive power at $(k+1)^{th}$ bus.

During the operation, the voltage level of the entire network must be increased by maximizing the bus with the lowest VSI value. As a result, the objective function for maximization of VSI is given as [51]:

$$\max F_3 = \frac{1}{min\left(VSI_{k+1}\right)} \tag{17}$$

C. OPERATIONAL CONSTRAINTS

The constraints subjected for the EVCS and DGs allocation in the radial distribution network are presented below.

1) EQUALITY CONSTRAINTS

a: ACTIVE AND REACTIVE POWER BALANCE

The active and reactive power delivered by electric substation and DG must be equal to the summation of APL, active and

reactive power demand, and additional CS load capacity.

$$P^{substation}+\sum_{k=1}^{N_{bus}} P^{DG}(k) = \sum_{j=1}^{N_{br}} P^{j}_{loss}(k,k+1) + \sum_{k=1}^{N_{bUS}} P_{D,k}+P^{k}_{EVCS} \quad (18)$$

$$Q^{substation}+\sum_{k=1}^{N_{bUS}} Q^{DG}(k) = \sum_{j=1}^{N_{br}} Q^{j}_{loss}(k,k+1) + \sum_{k=1}^{N_{bUS}} Q_{D,k} \quad (19)$$

where, $P^{substation} and Q^{substation}$ are the real and reactive power supplied by electric substation respectively, $P_{D,k} and Q_{D,k}$ are the active and reactive power demand at k^{th} bus, $P^{DG}(k)\, and Q^{DG}(k)$are the total real and reactive power injected by DGs at k^{th} bus, P^{j}_{loss} *and* Q^{j}_{loss} represents the real and reactive power loss in the j^{th} branch, P^{k}_{EVCS} is the charging station load at k^{th} bus and $N_{br} and N_{bus}$ denotes the number of branches and buses in the distribution network, respectively.

2) INEQUALITY CONSTRAINTS

a: VOLTAGE LIMIT CONSTRAINT

Each bus's voltage magnitude ranges between 0.95 to 1.05 p.u.

$$V_{min} \le V_k \le V_{max} k = 1, 2, 3 \ldots . N_{bus} \quad (20)$$

b: LINE CURRENT CONSTRAINT

The actual current flows in each line should not exceed the maximum limit of line current.

$$I_j \le I_j^{max} j = 1, 2, 3 \ldots . N_{br} \quad (21)$$

where, I_j represents the actual current flows in j^{th} line and I_j^{max} is the maximum limit of line current.

c: ACTIVE AND REACTIVE POWER INJECTED BY DG

The active and reactive power injected by DGs should lie within some specified limits.

$$P^{min}_{DG_k} \le P_{DG_k} \le P^{max}_{DG_k} \quad (22)$$

$$Q^{min}_{DG_k} \le Q_{DG_k} \le Q^{max}_{DG_k} \quad (23)$$

$P^{min}_{DG_k}$ and $P^{max}_{DG_k}$ are the minimum and maximum active power limits of k^{th} DG respectively and $Q^{min}_{DG_k}$ and $Q^{max}_{DG_k}$ are the minimum and maximum active power limits of k^{th} DG.

d: DG UNIT'S PENETRATION

$$\sum_{k=1}^{N_{DG}} P_{DG_k} \le \%J \times \sum_{k=1}^{N_{bus}} P_{L_k} \quad (24)$$

where J represents maximum DG unit penetration in the distribution system, N_{DG} is the number of DGs installed in the system.

III. THE HYBRID GREY WOLF–PARTICLE SWARM OPTIMIZATION (HGWOPSO) ALGORITHM

The EVCS and DG allocation problem is associated with discrete bus numbers, whereas capacity of DG unit is decided by operational constraints. GWO and PSO would not yield the same results after every iteration due to the stochastic behavior of the problem, exclusively in sophisticated systems. Therefore, it is a challenging task to investigate the optimum solution. On the other hand, the proposed hybrid approach HGWOPSO solves this issue. With the combination of GWO and PSO, a hybrid strategy is proposed. PSO's flaw is that it can't access the best answer across a large search area and is trapped in local optima. While GWO has the shortcoming of inefficient exploitation. Therefore, a combination of GWO and PSO is used to overcome the shortcomings of each method. The key ability is to combine the PSO's exploitation skills with the GWO's exploration capabilities in order to keep a proper exploration and exploitation to avoid local optima and arrive at an optimal solution with ease. HGWOPSO is presented in this work, in which GWO updates the initial population and then PSO updates the updated solutions [52]. Furthermore, the proposed hybrid approach is selected to efficiently tackle the optimization problem because it provides high-speed convergence and the capability of handling discrete as well as integer variable problems involving a smaller number of control parameters.

A. PARTICLE SWARM OPTIMIZATION (PSO) ALGORITHM

Kennedy and Eberhart, in 1995, devised the PSO as a nature-inspired optimization method [53]. PSO uses a swarm-based exploration method to find the global optimal. Its motivation is derived from the behavior of birds. The particles are taken and moved across the exploration area to search for the optimal population that solves the challenge. Particles are formed in a multidimensional exploration field, and each particle alters its location based on past knowledge and that of its neighbors. Also, particles are directed by the optimal location that they and their neighbors have reached [53]. The PSO's advantages are that it is simple to use and does not require numerous parameter modifications. The following rules can be used to adjust the position [54]:

$$\text{if x} > \text{pbestx}, \text{v}_\text{x} - \text{randxa}, \text{else } \text{v}_\text{x} = \text{v}_\text{x} + \text{randxa}$$

$$\text{if y} > \text{pbesty}, \text{v}_\text{y} - \text{randxa}, \text{else } \text{v}_\text{y} = \text{v}_\text{y} + \text{randxa}$$

where pbest denotes the highest position ever attained. rand signifies a random number lies between 0 and 1, and a is the position adjusting constant. The velocity must also be updated in accordance with the requirements below.

$$\text{if x} > \text{gbestx}, \text{v}_\text{x} = \text{v}_\text{x} - \text{randxb}, \text{else } \text{v}_\text{x} = \text{v}_\text{x} + \text{randxb}$$

$$\text{if y} > \text{gbesty}, \text{v}_\text{y} = \text{v}_\text{y} - \text{randxb}, \text{else } \text{v}_\text{y} = \text{v}_\text{y} + \text{randxb}$$

where gbest is the overall swarm's best location so far, and b is the constant for altering velocity.

B. GREY WOLF OPTIMIZATION (GWO) ALGORITHM

Mirjalili *et al.* are the ones who first introduced GWO in the year 2014 [55]. It takes its cues from the natural behavior and chasing method of grey wolves. They follow a strict leadership system in a pack. The group's leaders are known as alpha (α) wolves. Grey wolves are divided into two categories. The alpha comes under the first category, while the rest of the pack members are considered in the second category. They assist the alphas. The beta (β) wolves are their name. Furthermore, delta (δ) wolves have a lower priority than those of the previous two categories of wolves. Their goal is to surrender to alpha and beta wolves while maintaining influence over omega wolves. The omegas (ω) are the wolves with the lowest priority, as they must obey the foremost grey wolves. The mathematical representations of the GWO technique are as follows [55]:

1) SOCIAL HIERARCHY OF GREY WOLVES

Alpha wolf is known as the best suitable solution in the mathematical description of the grey wolf hierarchy. As a result, beta wolf is the second most acceptable solution, while delta is the third most suitable alternative. The omegas represent the farthest solutions. The hunting process is guided by alpha, beta, and delta in the GWO approach. The omegas should only follow the same steps as the wolves with higher priorities and obey them.

2) ENCIRCLING THE PREY

The grey wolves enclosing the prey while hunting. The encircling of grey wolves can be modeled using Eq. (25) and (26).

$$\overrightarrow{D} = \left|\overrightarrow{C}.\overrightarrow{X_p}(t) - \overrightarrow{X}(t)\right| \tag{25}$$

$$\overrightarrow{X}(t+1) = \overrightarrow{X_p}(t) - \overrightarrow{A}.\overrightarrow{D} \tag{26}$$

where t indicates the iteration, $\overrightarrow{A}$ and $\overrightarrow{C}$ represents the constant (coefficient) vectors, position vector of prey and wolf are represented by $\overrightarrow{X_p}$ and $\overrightarrow{X}$ respectively.

$\overrightarrow{A}$ and $\overrightarrow{C}$ can be formulated as follows:

$$\overrightarrow{A} = 2\overrightarrow{a}.\overrightarrow{r_1} - \overrightarrow{a} \tag{27}$$

$$\overrightarrow{C} = 2.\overrightarrow{r_2} \tag{28}$$

The value of $\overrightarrow{a}$ declines proportionally from two to zero over the entire iterations. $\overrightarrow{r_1}$ and $\overrightarrow{r_2}$ are the arbitrary random vectors taken between 0 and 1.

3) HUNTING MECHANISM OF GREY WOLVES

The alphas, betas, and deltas often drive the hunting process as they have more knowledge in predicting the location of the prey. The rest of the exploration mediators must follow the location of the optimal mediator and make adjustments as needed [56].

$$\overrightarrow{D_\alpha} = \left|\overrightarrow{C}.\overrightarrow{X_\alpha} - \overrightarrow{X}\right|; \overrightarrow{D_\beta} = \left|\overrightarrow{C}.\overrightarrow{X_\beta} - \overrightarrow{X}\right|; \overrightarrow{D_\delta} = \left|\overrightarrow{C}.\overrightarrow{X_\delta} - \overrightarrow{X}\right| \tag{29}$$

$$\overrightarrow{X_1} = \overrightarrow{X_\alpha} - \overrightarrow{A_1}.\overrightarrow{D_\alpha}; \overrightarrow{Z_2} = \overrightarrow{X_\beta} - \overrightarrow{A_2}.\overrightarrow{D_\beta}; \overrightarrow{X_3} = \overrightarrow{X_\delta} - \overrightarrow{A_3}.\overrightarrow{D_\delta} \tag{30}$$

$$\overrightarrow{X}(t+1) = \frac{\overrightarrow{X_1} + \overrightarrow{X_2} + \overrightarrow{X_3}}{3} \tag{31}$$

4) ATTACKING PROCESS OF GREY WOLVES

A is a number that falls between [−2a, 2a]. If |A| is greater than one, the wolves will attack their prey. Exploitation refers to the ability to attack the prey, while exploration is the skill of determining a prey. The population is led away from the prey by the erratic values of A. If |A| is greater than 1, the wolves will depart from their prey.

5) THE HGWOPSO ALGORITHM IMPLEMENTATION FOR EVCS AND DG ALLOCATION

Optimum allocation of DG units and the EVCS decreases system losses due to the addition of EVCS in the radial distribution system. It also improves voltage profile and stability. In this research analysis, EVCS and DG's allocation problems are addressed using the proposed HGWOPSO technique. Fig. 3. displays the flow chart of the suggested hybrid algorithm.

The steps mentioned below explain the working of the HGWOPSO algorithm.

Step 1: Initializing the maximum iterations.

Step 2: Initializing the number of search agents (NSA).

Step 3: Running GWO algorithm.

Step 4: The points minimized by GWO are passed through PSO as initial points.

Step 5: Running PSO algorithm.

Step 6: Updated points are passed back to the GWO algorithm.

Step 7: Increasing the iteration one by one.

Step 8: If the termination conditions are fulfilled, go to step 9; otherwise, go to step 3.

Step 9: The gbest solution is the desired solution of HGWOPSO technique.

The tuned parameters of the proposed HGWOPSO algorithm are NSA=30, swarm size=50, maximum iterations=100, inertia weight=0.4 to 0.9, and values of cognitive and social acceleration coefficients are 2.01 and 2.02, respectively.

IV. IMPACT OF EVCS AND DGS ON RELIABILITY OF DISTRIBUTION SYSTEM

The reliability study of the electrical distribution system has emerged as a demanding area of research. The possibility that a system will perform satisfactorily for a particular period under a specific set of operating constraints is referred to as reliability [14]. The reliability of generation, transmission, and distribution is prioritized in electrical network reliability studies. The amount of consumer satisfaction is strongly correlated to the distribution network's reliability. Quantitative data for the failure rate, repair rate, average outage duration, and the number of customers on load points of the distribution

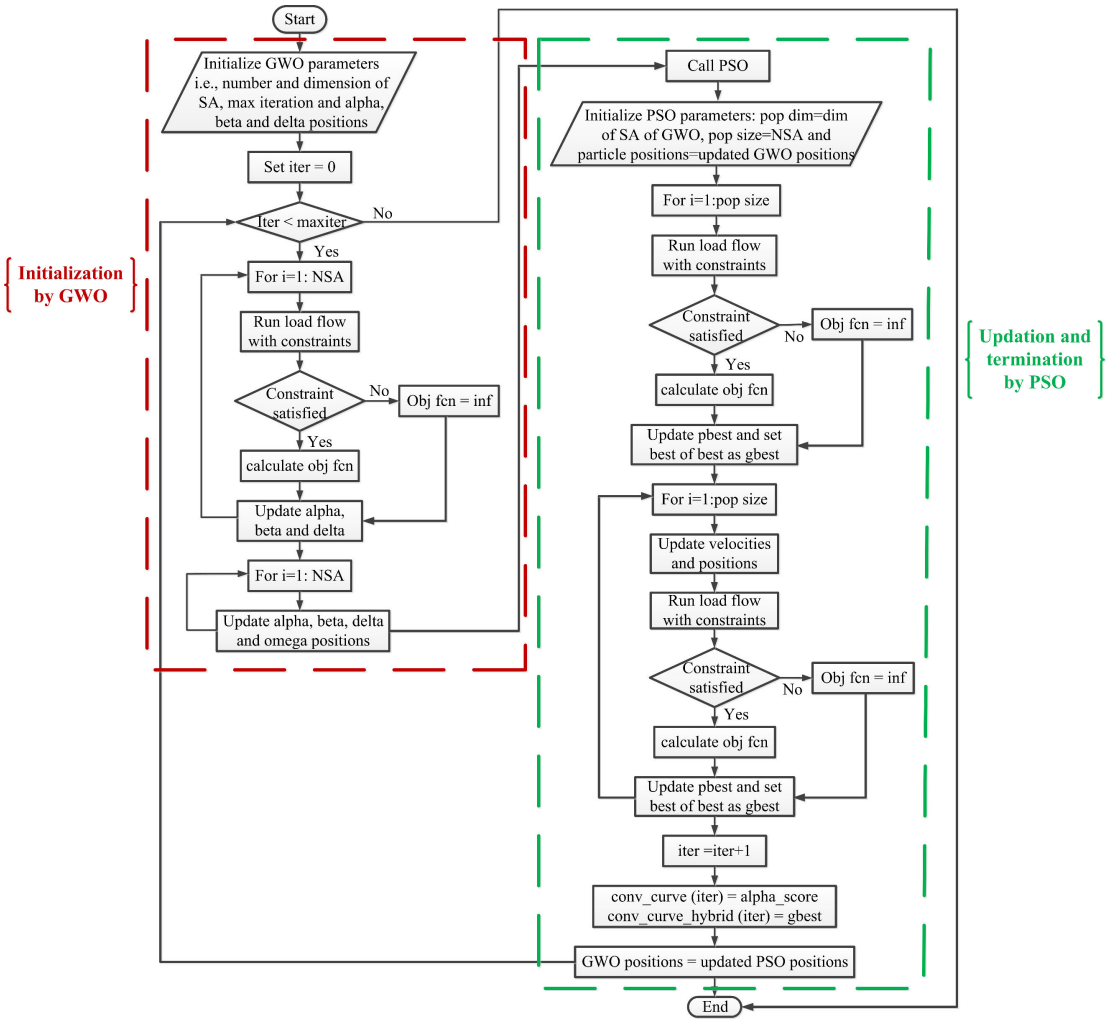

FIGURE 3. Flow chart of HGWOPSO.

network is needed to evaluate the distribution network's reliability indices [57]. Some of the reliability indices which are predominantly used to evaluate the system's reliability are SAIFI, SAIDI, CAIDI, EENS, AENS, ASAI, and ASUI. They are also employed in this research work to judge the reliability of the distribution system. An appropriate set of indices must be determined based on the application to attain the reliability evaluation.

A. CALCULATION OF STATISTICAL PARAMETERS FOR RELIABILITY AT DIFFERENT LOAD POINTS

The reliability indices strongly depend on various statistical parameters such as failure rate, repair rate, average outage duration. The reliability parameters can be calculated at different load points i.e., q^{th} load point as follows.

$$\text{Average failure rate } (\rho_q) = \sum_{k\in z} \text{num}_k \times \text{FR}_k \text{ failure/year}$$

$$\text{Annual outage duration } (U_q) = \sum_{k=z} \text{FR}_k D_{qk} \text{ hour/year}$$

$$\text{Average outage duration } (D_q) = \frac{U_q}{\rho_q} \text{ hour}$$

where FR_k is the average failure rate of the k^{th} element, z is the number of elements in the distribution system, num_k denotes the number of k^{th} elements in the distribution system, D_{qk} represents the period of failure at q^{th} load point due to failure of k^{th} element, ρ_q is the average failure rate at q^{th} load point and U_q denotes the annual outage duration at q^{th} load point.

B. FORMULAE OF RELIABILITY INDICES OF DISTRIBUTION SYSTEM

The reliability indices are characterized into load-oriented and customer-oriented indices. The complete categorization of reliability analysis of distribution system is depicted in Fig. 4.

A broad overview and mathematical formulae of different load and customer-oriented reliability indices are as follows [57].

1) CUSTOMER ORIENTED RELIABILITY INDICES

These indices have increased the reliability of power systems in terms of improving consumer or load facilities.

An extensive outline and mathematical formulae of different customer-oriented reliability indices are as follows.

The System Average Interruption Frequency Index (SAIFI) is calculated as the ratio of the total number of interruptions to the total number of customers served each year, as given in Eq. (32). SAIFI depicts the state of the system in terms of interruption. It is measured in failures/customers. year.

$$SAIFI = \frac{\sum_{q=1}^{z_q} \rho_q N_q}{\sum_{q=1}^{z_q} N_q} failures/customer.year \quad (32)$$

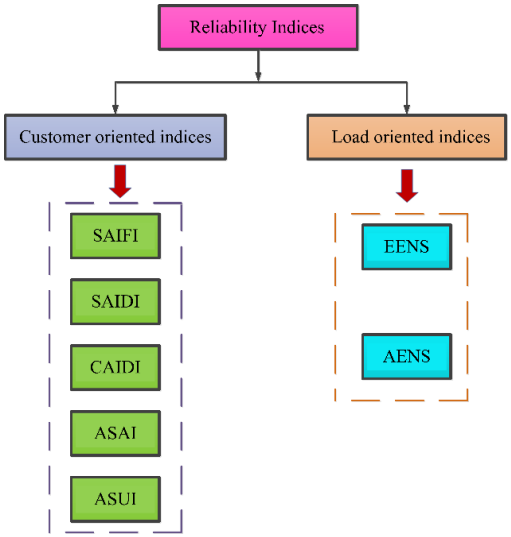

FIGURE 4. Categorization of reliability indices of distribution network.

The System Average Interruption Duration Index (SAIDI) is a fraction of total continuous interruptions divided by the number of customers served per year, as provided in Eq. (33). SAIDI depicts the state of the system in terms of interruption time. It is measured in hour per customer year.

$$SAIDI = \frac{\sum_{q=1}^{z_q} U_q N_q}{\sum_{q=1}^{z_q} N_q} hour\ per\ customer.year \quad (33)$$

The Customer Average Interruption Duration Index (CAIDI) is the ratio of the overall time of continuous interruptions to the total number of interruptions served by customers in a year, as shown in Eq. (34). CAIDI calculates the average outage time for any individual customer. It is measured in hour/customer. interruption.

$$CAIDI = \frac{SAIDI}{SAIFI}$$
$$CAIDI = \frac{\sum_{q=1}^{z_q} U_q N_q}{\sum_{q=1}^{z_q} \rho_q N_q} hour/customer.interruption \quad (34)$$

The Average Service Availability Index (ASAI) is expressed in per unit (p.u.). It is defined as the ratio of total available hours in a year to total desired hours, as specified in Eq. (35).

$$ASAI = \frac{\sum N_q \times 8760 - \sum_{q=1}^{z_q} U_q N_q}{\sum N_q \times 8760} (p.u) \quad (35)$$

The Average Service Unavailability Index (ASUI) is expressed in per unit (P.U.) and is defined as the ratio of total unavailable hours in a year to total desired hours, as specified in Eq. (36)

$$ASUI = 1 - ASAI\ (p.u) \quad (36)$$

2) ENERGY OR LOAD ORIENTED RELIABILITY INDICES

Load-oriented reliability indices are determined at different load points as follows.

The network's Expected Energy Not Supplied (EENS) is measured in MWh/year and equals the sum of all consumers' EENS as shown in Eq. (37). The EENS is an indication of energy insufficiency.

$$EENS_q = \sum \begin{bmatrix} (Demand\ at\ q^{th} load\ point) * \\ annual\ outage\ duration\ at\ q^{th} load\ point \end{bmatrix}$$
$$EENS_q = L_q U_q\ MWh\ per\ year \quad (37)$$

The Average Energy Not Supplied (AENS) index indicates how much energy isn't served within a given period, as shown in Eq. (38). It is expressed in MWh per customer per year.

$$AENS = \frac{\sum (EENS\ at\ q^{th} load\ point)}{Total\ number\ of\ customers\ at\ all\ load\ points}$$
$$AENS = \frac{\sum_{q=1}^{z_q} L_q U_q}{\sum_{q=1}^{z_q} N_q} MWh\ percustomer\ per\ year \quad (38)$$

where L_q is average demand/load at q^{th}loadpoint, $EENS_q$ denotes the expected ENS at q^{th}loadpoint, z_q is the total number of load points, N_q represents the total number of customers at q^{th} load point. The steps employed for the calculation of reliability indices is indicated in Fig. 5.

The interruption in power system network occurs due to following causes.

1) outages resulting in disturbance.
2) Failure of power system equipment leads to interruption.
3) Load shedding occurs due to abrupt rise in demand.
4) Planned preservation of equipment necessitating an interruption.

V. RESULTS AND DISCUSSION

This section describes the implementation of the proposed hybrid algorithm first on benchmark functions, and further, it is applied to the 33 and 69 bus systems. Also, the impact of EVCS and DG integration on the two considered standard systems in terms of reliability indices, i.e., SAIFI, SAIDI, CAIDI, etc., has been evaluated and explained in detail.

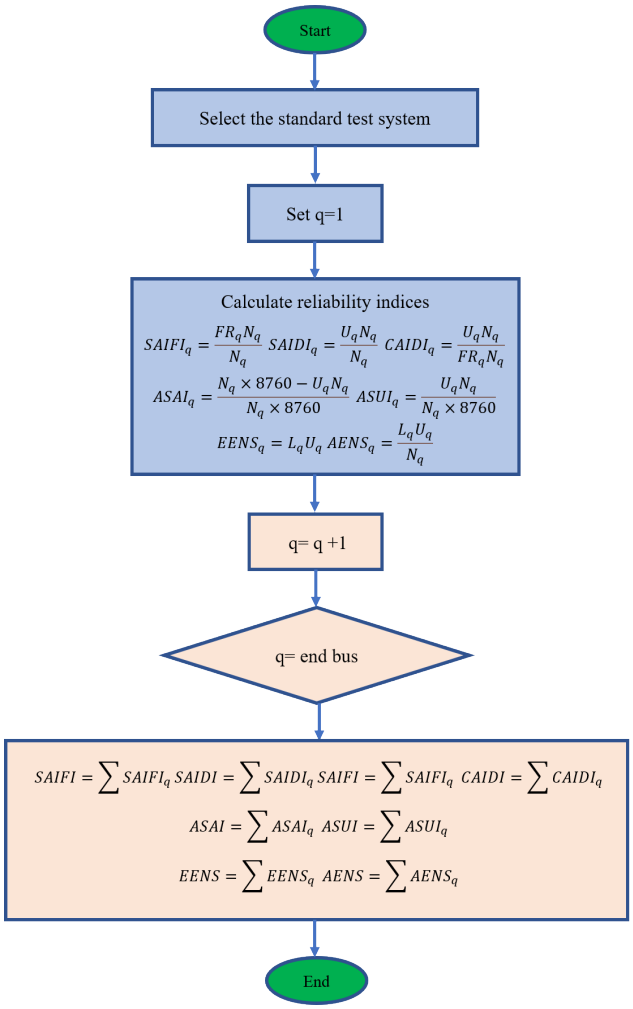

FIGURE 5. Flow chart for the computation of reliability indices.

A. PERFORMANCE OF PROPOSED ALGORITHM ON BENCHMARK FUNCTION

The proposed HGWOPSO is first applied to seven standard mathematical benchmark functions for validation. The complete details of these functions and their outcomes are provided in Tables 1 and 2, respectively. Comparative results in terms of maximum iterations and optimal solution of seven mathematical benchmark functions for 30 independent runs validate that the proposed optimization technique is superior to GWO and PSO. HGWOPSO converges to a global optimum without getting stuck in local optimal solution, resulting in faster convergence.

The suggested HGWOPSO is then employed in the IEEE 33-bus and 69-bus radial distribution systems for the location and sizing of EVCS and DG units. The results are compared with GWO and PSO for the single objective function corresponding to (1) minimizing the active power loss (2) minimization of voltage deviation (3) maximizing the voltage stability index. The proposed HGWOPSO algorithm is executed in MATLAB R2016a on an Intel i7, 3.2 GHz, 4 GB RAM, desktop PC.

B. IEEE-33 BUS BALANCED RADIAL DISTRIBUTION SYSTEM

The detailed diagram of IEEE 33 bus radial distribution system along with two DG and two EVCS is shown in Fig. 6. The IEEE-33 bus distribution network has 33 nodes and 32 branches. The system is allowed to operate at 100 MVA and 12.66 kV. It has total real power loads of 3715 kW and total reactive power loads of 2300 kVar. Charging stations are assumed to have 30 charging points, and each charger consumes 50 kW. So, CS can charge 30 EVs at the same time. The optimal number of CS needs to be placed at the optimal bus in the distribution network. Since CS installation increases the active power loss of the network. Hence, DGs are optimally placed to compensate for the losses due to installed EVCS. The power loss is optimized using the suggested HGWOPSO method. Before installing EVCS and DG, a direct approach-based load flow study is carried out to determine the base case losses. The active and reactive power values before installing EVCS and DGs are observed to be 201.9 kW and 134.7 kVAr, respectively. Also, the minimum voltage appears at bus 18 of magnitude 0.9131 p.u. Whereas the minimum value of VSI comes out to be 0.6953 p.u.

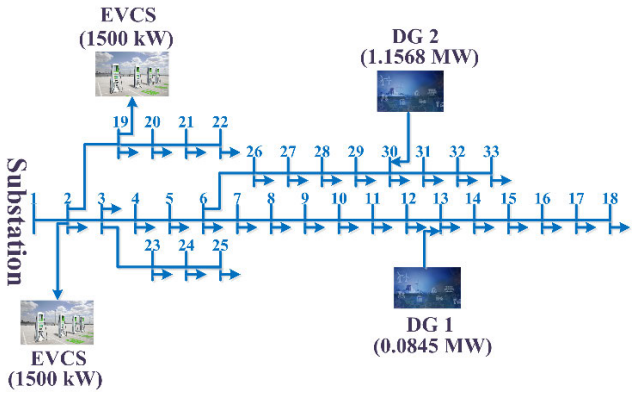

FIGURE 6. Connection diagram of IEEE 33-bus system with two EVCS and two DGs.

1) EFFECT OF EVCS AND DG INTEGRATION ON SYSTEM LOSS IN 33-BUS SYSTEM

The addition of EVCS to the distribution network raises the APL while lowering the voltage profile due to the increased loading of EVs. Therefore, there is a requirement to allocate the EVCS in the most efficient way possible, resulting in the lowest possible rise in APL. It's worth noting that installing a fixed capacity EVCS on bus 2 results in a power loss of only 211.7 kW. To meet customer demand and ensure the availability of EVCS for EV users, an increasing number of EVCS must be installed to address the power loss issues. The best placement of the second EVCS at bus 19 results in a total active power loss of 214.8 kW.

Five different scenarios are addressed in this work for validating the methodology. The scenarios are given below:

Scenario 1: Balanced IEEE 33-bus radial distribution network with existing loads only

TABLE 1. List of standard mathematical benchmark functions.

S. No	Function Name	Mathematical Formulation	Dimension (D)	Search Range
1.	Sphere	$f(x)=\sum_{p=1}^{D} x_p^2$	30	[-100,100]
2.	Rosenbrock	$f(x)=\sum_{p=1}^{D}\left[100*\left(x_p^2-x_{p+1}\right)^2+\left(1-x_p\right)^2\right]$	30	[-2.048,2.048]
3.	Rastragin	$f(x)=\sum_{p=1}^{D}\left[x_p^2-10\cos\left(2\pi x_p\right)+10\right]$	30	[-5.12,5.12]
4.	Greiwank	$f(x)=\frac{1}{4000}\sum_{p=1}^{D} x_p^2-\prod_{p=1}^{D} cos\left(\frac{x_p}{\sqrt{p}}\right)+1$	30	[-600,600]
5.	Schewefel	$f(x)=\sum_{p=1}^{D}\left(\sum_{q=1}^{p} x_q\right)^2$	30	[-100,100]
6.	Ackley	$f(x)=-20e^{\left(-0.2\sqrt{\frac{1}{D}\sum_{p=1}^{D} x_p^2}\right)}-e^{\left(\frac{1}{D}\sum_{p=1}^{D}\cos(2\pi x_p)\right)}+20+e^1$	30	[-32.76,32.76]
7.	Alpine	$f(x)=\sum_{p=1}^{D-1}\left\|x_p sinx_p+0.1x_p\right\|$	30	[-10, 10]

TABLE 2. Comparison of results obtained from HGWOPSO, GWO and PSO applied on standard benchmark functions.

Function Name	HGWOPSO		GWO		PSO	
	Maximum Iterations	Optimal Solution	Maximum Iterations	Optimal Solution	Maximum Iterations	Optimal Solution
Sphere	1000	$1.55*10^{-22}$	897	$5.89*10^{-20}$	1000	$7.25*10^{-19}$
Rosenbrock	425	$2.72*10^{-2}$	515	$5.81*10^{1}$	548	$4.57*10^{2}$
Rastragin	343	$7.57*10^{-13}$	419	$5.53*10^{-9}$	495	$2.53*10^{-2}$
Greiwank	1000	$4.25*10^{-2}$	1000	$3.45*10^{-2}$	1000	$2.87*10^{-1}$
Schewefel	1000	8592.7	1000	7956.4	1000	6985.8
Ackley	1000	$7.74*10^{-9}$	785	$9.14*10^{-5}$	1000	$8.54*10^{-3}$
Alpine	1000	-192.55	1000	-192.45	1000	-192.50

Scenario 2: Addition of one EVCS in radial distribution network

Scenario 3: Addition of one more EVCS in distribution network

Scenario 4: Addition of one DG in radial distribution network

Scenario 5: Simultaneous allocation of two DGs

The placement of DG in an optimal location with an optimal size result in minimization of APL, improvement in voltage profile, and enhancement in VSI. A large number of research articles has focused on minimizing APL due to the domination of I^2R losses in the power system. The APL, VDI, and VSI are calculated before the reliability evaluation. This is done to evaluate the reliability of the system by determining the best DG size, DG location, power loss, VDI, and VSI.

Two DGs are installed in the 33 bus network to reduce the charging impact of EVs. When one 2.56 MW DG is optimally located at bus 6, it results in a 103.6 kW active power loss. The power loss is reduced to 85.5 kW when two DGs with capacities of 0.0845 MW and 1.1568 MW are situated optimally at bus numbers 13 and 30 in the distribution network. Table 3. illustrates the APL values when EVCS and DGs are installed sequentially in 33 bus distribution networks.

TABLE 3. APL values after the placement of EVCS and DGs using HGWOPSO in 33-bus system.

Scenarios	Bus number and size	APL (kW)
Base case	-	201.9
1 EVCS	1500 kW at bus 2	211.7
2 EVCS	1500 kW at bus 2 and 19	214.8
1 DG	2.56 MW at bus 6	103.6
2 DGs	0.0845 MW and 1.1568 MW at bus 13 and 30	85.5

Also, the varying power loss values after placing EVCS and DGs are depicted in Fig. 7. The comparison analysis of the size and location of EVCS and DG and their impact on power loss is portrayed in Table 4. Also, it is realized from Table 4 that results obtained by implementing HGWOPSO

TABLE 4. Comparison of optimal size, location and APL of EVCS and DG obtained using HGWOPSO, GWO and PSO for 33-bus system.

Scenarios	HGWOPSO				GWO				PSO			
	EVCS Location	Optimal DG		APL (kW)	EVCS Location	Optimal DG		APL (kW)	EVCS Location	Optimal DG		APL (kW)
		Location	Size (MW)			Location	Size (MW)			Location	Size (MW)	
Base case	-	-	-	201.9	-	-	-	202.2	-	-	-	204.7
1 EVCS	2	-	-	211.7	2	-	-	213.9	2	-	-	214.5
2 EVCS	2, 19	-	-	214.8	2, 19	-	-	215.6	2, 19	-	-	216.2
1 DG	2, 19	6	2.56	103.6	2, 19	8	2.71	105.7	2, 19	6	2.78	107.2
2 DGs	2, 19	13	0.0845	85.5	2, 19	17	0.0978	87.1	2, 19	13	1.1024	88.7
		30	1.1568			29	1.2193			30	1.3421	

are superior to GWO and PSO for the same parameter consideration.

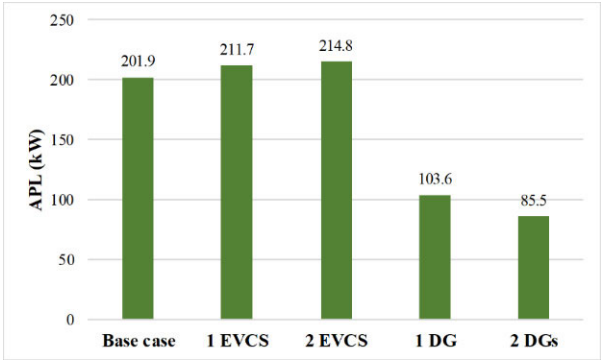

FIGURE 7. Effect of EVCS and DG integration on active power loss in 33-bus system.

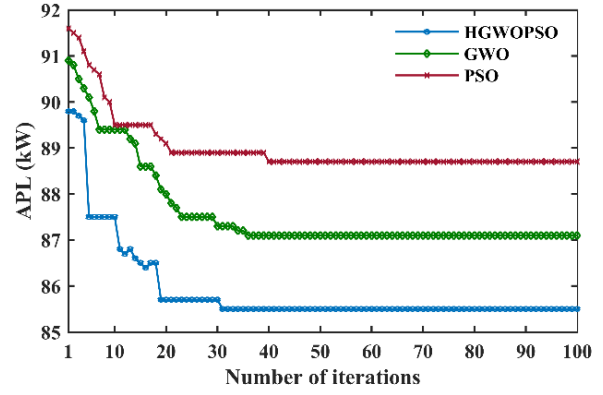

FIGURE 8. Convergence plot for active power loss using HGWOPSO, GWO, and PSO in 33-bus network.

Likewise, the efficacy of the proposed hybrid technique, i.e., HGWOPSO, is confirmed by comparing the obtained results with those of other existing techniques such as GWO and PSO.

The proposed technique results in active power loss of 85.5 kW which is lesser than those of GWO (87.1 kW) and PSO (88.7 kW). Fig. 8. shows the converging nature of the active power loss over the course of iteration using proposed HGWOPSO, GWO, and PSO. Also, it is evident from the convergence characteristics that HGWOPSO has a faster rate of achieving optimal solutions as compared to standalone GWO and PSO.

2) EFFECT OF EVCS AND DG INTEGRATION ON VOLTAGE PROFILE AND VOLTAGE STABILITY INDEX IN 33-BUS SYSTEM

As similar to system loss, integration of EVCS imposes a detrimental effect on the voltage profile and VSI. Due to the increased loading of EVs, the system's voltage profile and voltage stability index deteriorates. These disturbances are compensated by the suitable incorporation of DG units at appropriate node in the distribution system. The voltage profile of the 33- bus system when multiple EVCS and DGs are sited in the system is depicted in Fig. 9.

The voltage at each bus continues to decrease as the charging load grows, as seen in Fig. 9. When one 1500 kW EVCS is optimally placed on bus 2, the voltage profile of the entire system falls. Furthermore, as the number of EVCS grows, the voltage profile degrades.

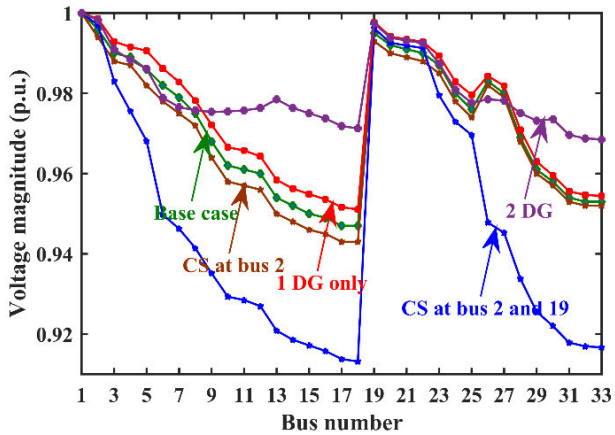

FIGURE 9. Voltage profile of 33 bus system after integrating EVCS and DG units.

DGs are integrated into the distribution system along with EVCS to ensure that the system runs smoothly. Integration of DG units creates positive impacts on the voltage profile of the system. Improvement in voltage profile after incorporating

DG units is shown in Fig. 9. The voltages on all the buses fluctuate depending on the distribution system's actual and reactive power losses. As a result, real power support is required for real power loss reduction, which enhances voltage levels by mitigating I^2R losses. Also, it is observed that the improvement in bus voltages takes place when many DGs are located. Also, it is noted that the size of a single DG is greater than the combined size of two DG units. In the case of one DG, the minimum magnitude of voltage is 0.9511 p.u at bus number 18; for simultaneous allocation of two DG units, the minimum voltage is improved to 0.9685 p.u at bus 33. So, it is deduced that minimum voltage improves with the employment of multiple DGs.

The addition of EVCS and DG units to the distribution network impacts the voltage stability index as it does on the voltage profile. The base case (before installing EVs and DGs) value of VSI is 0.6953 p.u. It drops to 0.6924 p.u when one EVCS of capacity 1500 kW is optimally installed at bus number 2. DGs implementation in distribution networks enhances the VSI. It can be noticed from Fig. 10. that VSI enhances when a greater number of DGs are situated optimally in the distribution system.

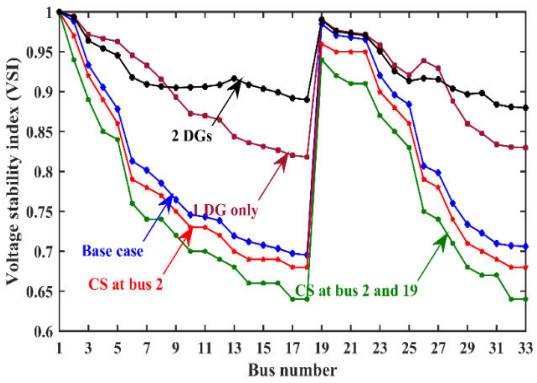

FIGURE 10. VSI for 33 bus system for different scenarios.

When one DG is placed causes the VSI to be increased to the value of 0.8181 p.u. Similarly, VSI becomes 0.8798 p.u. on the implementation of two DGs. Also, VSI is investigated for different scenarios using the suggested hybrid technique and compared to other techniques in order to demonstrate its superiority. The VSI results obtained using the two techniques for the 33-bus system are tabulated in Table 5.

TABLE 5. Comparison Of VSI Values For Different Scenarios In 33-Bus System.

Scenarios	HGWOPSO		GWO		PSO	
	VSI (p.u.)	Inverse VSI	VSI (p.u.)	Inverse VSI	VSI (p.u.)	Inverse VSI
Base case	0.695	1.438	0.691	1.447	0.6893	1.451
1 EVCS	0.692	1.444	0.689	1.451	0.6857	1.458
2 EVCS	0.681	1.467	0.679	1.472	0.6723	1.487
1 DG	0.818	1.222	0.807	1.239	0.7981	1.252
2 DGs	0.879	1.136	0.853	1.172	0.8343	1.198

C. IEEE-69 BUS BALANCED RADIAL DISTRIBUTION SYSTEM

The proposed algorithm HGWOPSO is now implemented on IEEE 69-bus radial DS for the optimal allocation of EVCS and DG. The detailed diagram of the IEEE 69-bus distribution system is shown in Fig. 11. Two fixed capacity EVCS and three type 1 DG have been considered. The details of the IEEE 69-bus DS are as follows: The IEEE-69 bus DS has 69 nodes and 68 branches. The system is allowed to operate at 100 MVA and 12.66 kV. It has total real power loads of 3801.4 kW and total reactive power loads of 2693.6 kVAr. As that of IEEE 33-bus radial distribution system, the objective functions, i.e., power loss minimization, improvement in voltage profile, and maximizing VSI, are optimized using HGWOPSO and compared with those of GWO and PSO.

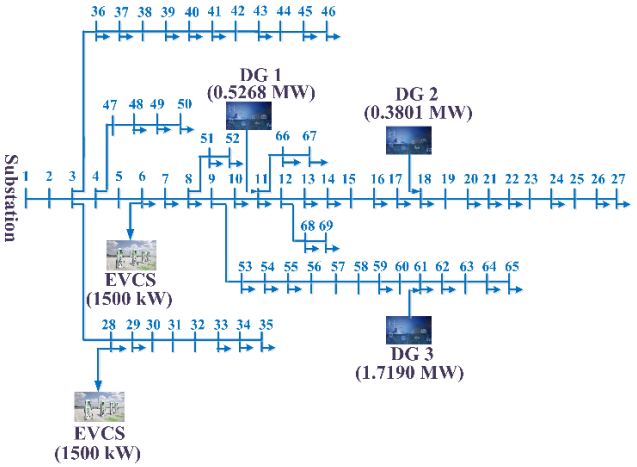

FIGURE 11. Connection diagram of IEEE 69-bus system with two EVCS and three DGs.

To validate the methodology for the proposed work, the following scenarios are considered.

Scenario 1: Balanced IEEE 69-bus radial DS with existing loads only

Scenario 2: Addition of one EVCS in radial distribution network

Scenario 3: Addition of one more EVCS in distribution network

Scenario 4: Addition of one DG in radial distribution network

Scenario 5: Simultaneous allocation of two DGs

Scenario 6: Simultaneous allocation of three DGs

1) EFFECT OF EVCS AND DG INTEGRATION ON SYSTEM LOSS IN 69-BUS SYSTEM

The base case active and reactive power loss in the 69-bus system is calculated to be 224.9 kW and 102.1 kVAr respectively. Similar to the 33-bus system, the addition of EVCS creates power loss issues in the 69-bus system. When one EVCS is optimally installed at bus 28 results in an active power loss of 225.31 kW. It is recommended to install the large number of charging infrastructures on the way of EV users

to increase the wide adoption of EVs. To this end, one more EVCS is placed at bus 6, which leads to a further increment in power loss of 254.45 kW. It is realized that the addition of charging infrastructures is essential for the survival of EVs but at the same time causes detrimental effects on the health of power system. Thus, compromise has to be made between the power system health and charging infrastructure. DGs are added to reduce the charging impact of EVs. However, the implementation of DGs on optimal nodes compensates for the power loss issues. In this context, when one DG of 1.8726 MW capacity is optimally placed at bus 61 results in an active power loss of 83.2 kW. When two DGs are located at buses 17 and 61, their sizes are 0.5312 MW and 1.7815 MW, respectively, providing a reduced APL of 71.7 kW. Also, APL is reduced to the value of 69.4 kW when three DGs with sizes 0.5268 MW, 0.3801 MW, and 1.7190 MW are installed at bus numbers 11, 18, and 61, respectively. When EVCS and DGs are placed successively in a 69-bus distribution network, the APL values are shown in Table 6.

TABLE 6. APL Values After The Placement Of EVCS And Dgs Using HGWOPSO in 69-bus system.

Scenarios	Bus number and size	APL (kW)
Base case	-	224.9
1 EVCS	1500 kW at bus 28	225.31
2 EVCS	1500 kW at bus 6 and 28	254.45
1 DG	1.8726 MW at bus 61	83.2
2 DGs	0.5312 MW and 1.7815 MW at bus 17 and 61	71.7
3 DGs	0.5268 MW, 0.3801 MW and 1.7190 at bus 11, 18 and 61	69.4

Table 7 shows a comparison of the size and placement of EVCS and DG, as well as their impact on power loss. In addition to this, Fig. 12. shows the varied power loss values after installing EVCS and DGs.

The efficacy of the suggested hybrid technique, HGWOPSO, is also proven by comparing the acquired findings to those of other existing techniques like GWO and PSO.

The proposed technique results in an active power loss of 69.4 kW, which is lower than the 70.5 kW and 71.7 kW incurred by GWO and PSO respectively.

Fig. 13. depicts the converging nature of active power loss throughout the duration of iteration using proposed HGWOPSO, GWO, and PSO. In addition, the convergence curve clearly shows that HGWOPSO achieves optimal solutions faster than isolated GWO and PSO.

2) EFFECT OF EVCS AND DG INTEGRATION ON VOLTAGE PROFILE AND VOLTAGE STABILITY INDEX IN 69-BUS SYSTEM

The addition of EVCS disrupts the voltage profile of this system, which is similar to that of a 33-bus network. The minimal voltage of magnitude 0.9091 p.u. exists at bus 65 in the base case. When EVCS is installed at bus 28, the minimum voltage value is dropped to 0.9015, which occurs at bus 65. When

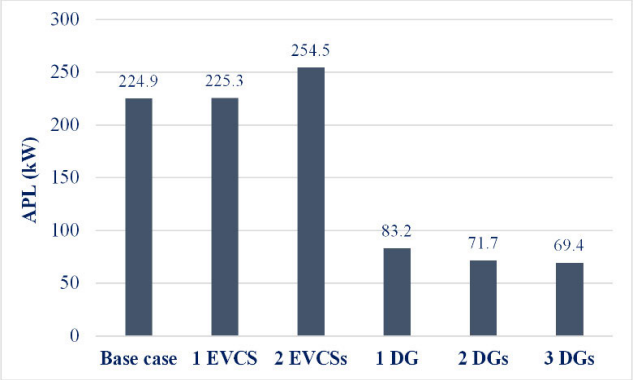

FIGURE 12. Effect of EVCS and DG integration on active power loss in 69-bus system.

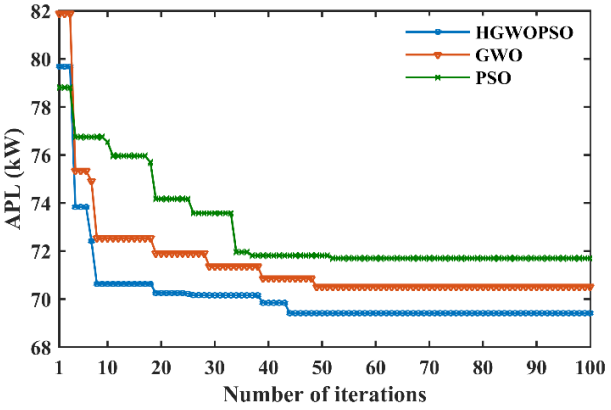

FIGURE 13. Convergence plot for active power loss using HGWOPSO, GWO and PSO in 69-bus network.

one more EVCS is added to node 6, the minimum voltage drops even lower to 0.8997 p.u. As a result, EVCS installation degrades the voltage profile of the system. DG units are integrated along with EVCS to maintain a healthy voltage profile. The voltage profile improves with the incorporation of DG units. In the case of one DG only, the minimum voltage is improved to 0.9683 p.u. at bus 27. When two DGs are optimally placed, the minimum voltage value comes out to be 0.9789 p.u. at bus 65. Moreover, simultaneous allocation of DG units further improves the bus voltage, i.e., the minimum voltage of 0.9790 p.u. at bus 65. Fig. 14. shows the voltage profile of the 33-bus system when EVCS and DGs are integrated.

VSI is influenced in the same way as voltage profile with the gradual increase of charging loads. The value of VSI before integrating EVCS is observed to be 0.6833 p.u. but it is decreased to 0.6709 p.u when charging load is added on bus 28. In the same way, VSI further drops to 0.6615 p.u with the addition of another EVCS at bus 6. Thus, the incorporation of charging infrastructures badly affects the system in terms of VSI. This problem is compensated by the integration of DGs into the distribution network. VSI improves to 0.8792 p.u. in the presence of one DG only. Further improvement in VSI takes place with the incorporation of

TABLE 7. Comparison Of Optimal Size, Location And APL Of EVCS And DG Obtained Using HGWOPSO, GWO And PSO For 69 Bus System.

Scenarios	HGWOPSO				GWO				PSO			
	EVCS Location	Optimal DG		APL (kW)	EVCS Location	Optimal DG		APL (kW)	EVCS Location	Optimal DG		APL (kW)
		Location	Size (MW)			Location	Size (MW)			Location	Size (MW)	
Base case	-	-	-	224.9	-	-	-	225.7	-	-	-	227.4
1 EVCS	28	-	-	225.31	28	-	-	227.67	-	-	-	229.17
2 EVCS	6, 28	-	-	254.45	6, 28	-	-	257.89	-	-	-	258.68
1 DG	6, 28	61	1.8726	83.2	6, 28	61	1.9536	85.9	1.9536	61	1.9536	87.5
2 DGs	6, 28	17 61	0.5312 1.7815	71.7	6, 28	17 61	0.7134 1.9235	72.5	0.7134 1.9235	17 61	0.7134 1.9235	73.8
3 DGs	6, 28	11 18 61	0.5268 0.3801 1.7190	69.4	6, 28	13 21 67	0.5312 0.3876 1.8138	70.5	0.5358 0.3952 1.8749	11 18 61	0.5358 0.3952 1.8749	71.7

TABLE 8. Comparison Of VSI Values For Different Scenarios In 69-Bus System.

Scenarios	HGWOPSO		GWO		PSO	
	VSI (p.u.)	Inverse VSI	VSI (p.u.)	Inverse VSI	VSI (p.u.)	Inverse VSI
Base case	0.683	1.463	0.672	1.488	0.6793	1.472
1 EVCS	0.670	1.491	0.664	1.506	0.6546	1.527
2 EVCS	0.661	1.511	0.648	1.543	0.6358	1.572
1 DG	0.879	1.137	0.871	1.148	0.8647	1.156
2 DGs	0.908	1.101	0.892	1.121	0.8957	1.116
3 DGs	0.918	1.089	0.911	1.097	0.9089	1.100

TABLE 9. Consumer Information At Different Load Points For 33-Bus System [14].

Number of load points	LOAD POINTS	Number of customers (consumers)
1	2	26
7	3, 18, 19, 20, 21, 22, 23	23
3	4, 14, 29	31
11	5, 6, 12, 13, 15, 16, 17, 26, 27, 28, 33	16
2	7, 8	52
2	9, 10	15
2	24, 25	109
1	11	12
1	30	25
1	31	39
1	32	35

more DG units. Integration of two DGs improves the VSI to 0.9083 p.u. While in the case of three DGs, it becomes 0.9185 p.u. In regard to this, improvement in VSI is seen in Fig. 15. by incorporating DGs.

In addition, VSI is explored for various scenarios using the recommended technique and compared to other techniques in order to establish its superiority. The VSI findings for the 69-bus system obtained using the two techniques are shown in Table 8.

D. EFFECT OF INTEGRATED EVCS AND DGs ON RELIABILITY OF 33 BUS AND 69 BUS DISTRIBUTION NETWORKS

The reliability indices are obtained to demonstrate the consequence of integrating EVCS and DG units on the system reliability. The reliability indices for the electrical network are calculated considering quantitative information about failure and repair rate, average outage time and number of customers at each load points. The reliability indices considered in this article are SAIFI, SAIDI, CAIDI, EENS, AENS, ASAI, and ASUI.

TABLE 10. Statistical Input Parameters At Different Load Points For 33-Bus System [14].

Load Point	Failure rate (Failure per year)	Outage duration (Hour per year)
2	0.05	0.03
3	0.04	0.03
4	0.06	0.03
5	0.03	0.02
6	0.03	0.02
7	0.09	0.6
8	0.03	0.6
9	0.03	0.2
10	0.02	0.2
11	0.03	0.1
12	0.03	0.2
13	0.06	0.2
14	0.03	0.3
15	0.03	0.2
16	0.03	0.2
17	0.03	0.2
18	0.04	0.2
19	0.04	0.2
20	0.04	0.2
21	0.04	0.2
22	0.04	0.2
23	0.04	0.2
24	0.19	1.1
25	0.19	1.1
26	0.03	0.2
27	0.03	0.2
28	0.03	0.2
29	0.54	0.3
30	0.09	0.5
31	0.07	0.4
32	0.1	0.6
33	0.03	0.2

1) RELIABILITY ANALYSIS FOR 33-BUS SYSTEM

The major goal of this section is to offer a detailed examination of the impact of the EV charging station and DG

TABLE 11. Effect Of EVCS And DGs Integration On Different Reliability Indices In 33 Bus System.

Scenarios	SAIFI	SAIDI	CAIDI	EENS	AENS	ASAI	ASUI
Base case	0.0982	0.5048	5.1385	1780	1.9369	0.9999	0.0001
1 EVCS	0.1195	0.6321	5.2915	9430.04	10.2612	0.9997	0.0003
2 EVCS	0.1361	0.7155	5.2558	15029.9	16.3547	0.9994	0.0007
1 DG	0.1217	0.5238	4.304	8765.46	9.5381	0.9997	0.0003
2 DGs	0.1147	0.4914	4.2842	6517.23	7.0946	0.9998	0.0002

TABLE 12. Statistical Input Parameters At Different Load Points For 69-Bus System [58].

Load Point	Failure rate (Failure per year)	Outage duration (Hour per year)
2, 52, 53, 54, 55, 56, 68, 69	0.221	1.94
3, 4, 35, 36, 37, 38, 39, 40, 41, 42, 43, 44, 45, 46, 47, 48	0.321	11.04
5, 8, 9, 11, 12, 29, 30, 14, 16, 18, 19, 20, 21, 22, 25, 27, 28	0.301	11.44
13, 15, 49, 50, 51, 62, 63, 64, 65	0.314	11.17
17, 23, 24, 57, 58, 59, 60, 61	0.208	1.75
31, 32, 33, 34, 66, 67	0.327	10.96

TABLE 13. Consumer Information At Different Load Points For 69-Bus System [58].

Number of load points	Load Points	Number of customers (consumers)
8	2, 3, 4, 5, 52, 53, 54, 55, 56	148
6	8, 9, 57, 58, 59, 60	10
9	11, 12, 62, 63, 64, 65, 66, 67, 68	132
4	13, 14, 15, 69	110
2	16, 61	2
5	17, 18, 19, 20, 50	118
20	21, 22, 23, 24, 25, 26, 35, 36, 37, 38, 39, 40, 41, 42, 43, 44, 45, 46, 47, 48	126
6	27, 28, 29, 30, 31, 49	108
4	32, 33, 34, 51	58

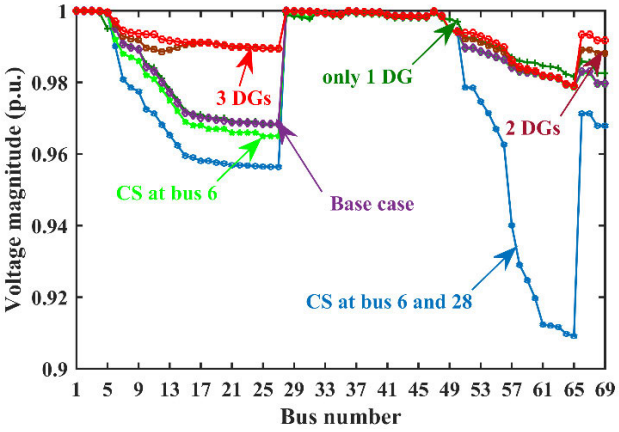

FIGURE 14. Voltage profile of 69 bus system after integrating EVCS and DG units.

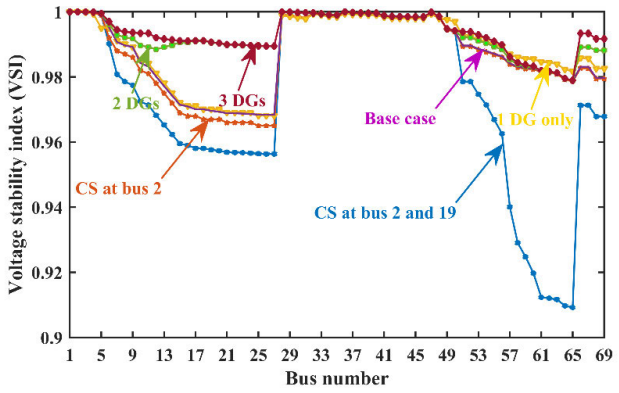

FIGURE 15. VSI for 69 bus system for different scenarios.

placement on the IEEE 33 bus system's reliability. Reliability indices are estimated for all the above-mentioned scenarios, i.e., after the placement of EVCS and DGs. Customer information and other statistical parameters such as failure rate, repair rate, and average outage time for the 33-bus system are stated in Table 9 and Table 10, respectively.

Both consumer and load (energy) oriented indices deteriorate after the installation of EVCS. On the other hand DGs integration into the distribution system enhances both types of reliability indices. This is due to the fact that DGs enable immediate and efficient bus voltage management, which improves power transfer capability and reduces power loss by regulating supplied power to the system. They also directly alter the power flow by controlling injected power. It is realized from Table 11 that the value of reliability indices worsens after the allocation of EVCS. The value of SAIFI before installing EVCS and DG, i.e., base case is 0.0982 failures/customer. year. After installing a fast-charging station with 30 charging points on bus 2, the SAIFI increased to 0.1195 failures/customer. year. The value of SAIDI and CAIDI also increased to 0.6321 hour per customer. year and 5.2915 hour/customer. interruption when one EVCS is allocated at bus 2. Likewise, deprivation of EENS and AENS is also observed in the case of one CS placement. The base value of AENS is 1.9369 MWh per customer per year. Its value increased to 10.2612 MWh per customer per year after the integration of one EVCS. As the EVCS is integrated into the distribution network, the energy is supplied to meet the load requirement, and thus, the indices associated with the energy not supplied are increased. The increment in reliability indices is not desirable from the perspective of the distribution system. Also, the value of ASAI decreases with the incorporation of charging loads. It refers to the condition that the availability of electricity decreases with increasing charging loads. Further, all reliability indices are evaluated when two EV charging loads

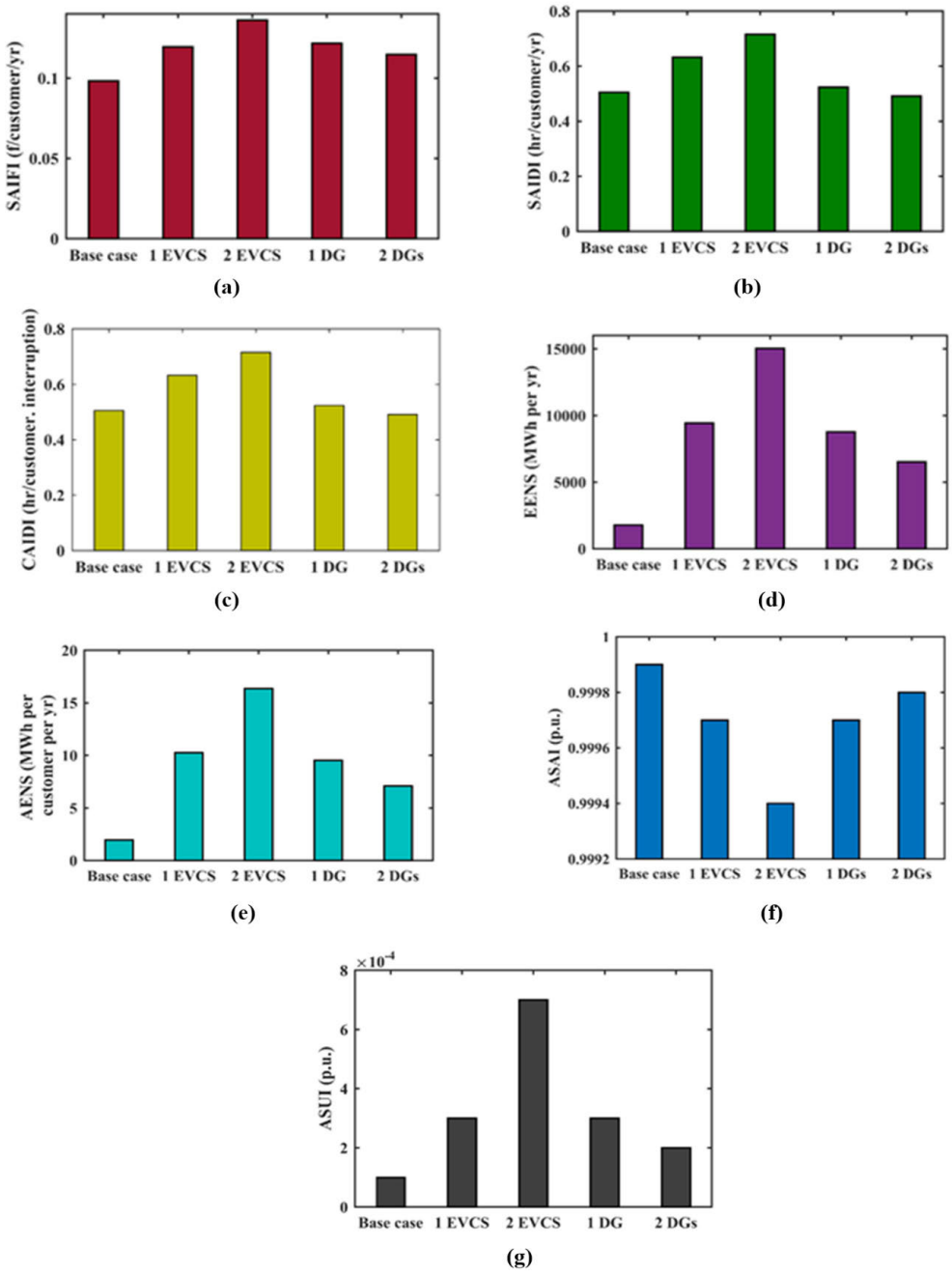

FIGURE 16. Variation in reliability indices with integration of EVCS and DGs in 33-bus system.

are placed at buses 2 and 19. When two charging station loads are shared between two nodes, the reliability is higher than when the two charging stations are concentrated on a single node. In some circumstances, when strong nodes of the electrical power network and high-traffic-density nodes of the transportation network merge, the paths connecting to that node become too crowded. As a result, distributing the charging stations has the added benefit of making the charging capability available to a broader number of EVs traveling in diverse routes, minimizing overcrowding of traffic on the particular paths leading to the bus where charging loads are concentrated.

Thus, it is desirable to inject some amount of energy into the distribution system to improve its reliability. One of the alternatives is to make use of DGs, which injects active and reactive power into the system depending on the requirement. Multiple DGs are optimally integrated into the network, which enhances the system's reliability. All reliability indices are investigated after integrating DGs. The impact of DGs integration on reliability indices is shown in Table 11. After the placement of one DG at bus 6, the value of SAIFI decreased to 0.1217 failures/customer. year. Similarly, the values of SAIDI and CAIDI also decreased to 0.5238 hour per customer. year and 4.304 hour/customer.

TABLE 14. Effect Of EVCS And DGs Integration On Different Reliability Indices In 69 Bus System.

Scenarios	SAIFI	SAIDI	CAIDI	EENS	AENS	ASAI	ASUI
Base case	2.4795	77.6787	31.3283	27195.51	33.4921	0.9911	0.0089
1 EVCS	2.4919	79.8148	31.9796	37006.33	45.5743	0.9908	0.0092
2 EVCS	2.5159	82.4789	32.7845	46967.21	57.8414	0.9906	0.0094
1 DG	2.5043	81.4879	32.5391	41857.06	51.5481	0.991	0.009
2 DGs	2.4951	80.8794	32.4153	35688.78	43.9517	0.9916	0.0084
3 DGs	2.4847	78.4879	31.5884	32487.54	40.00929	0.9925	0.0075

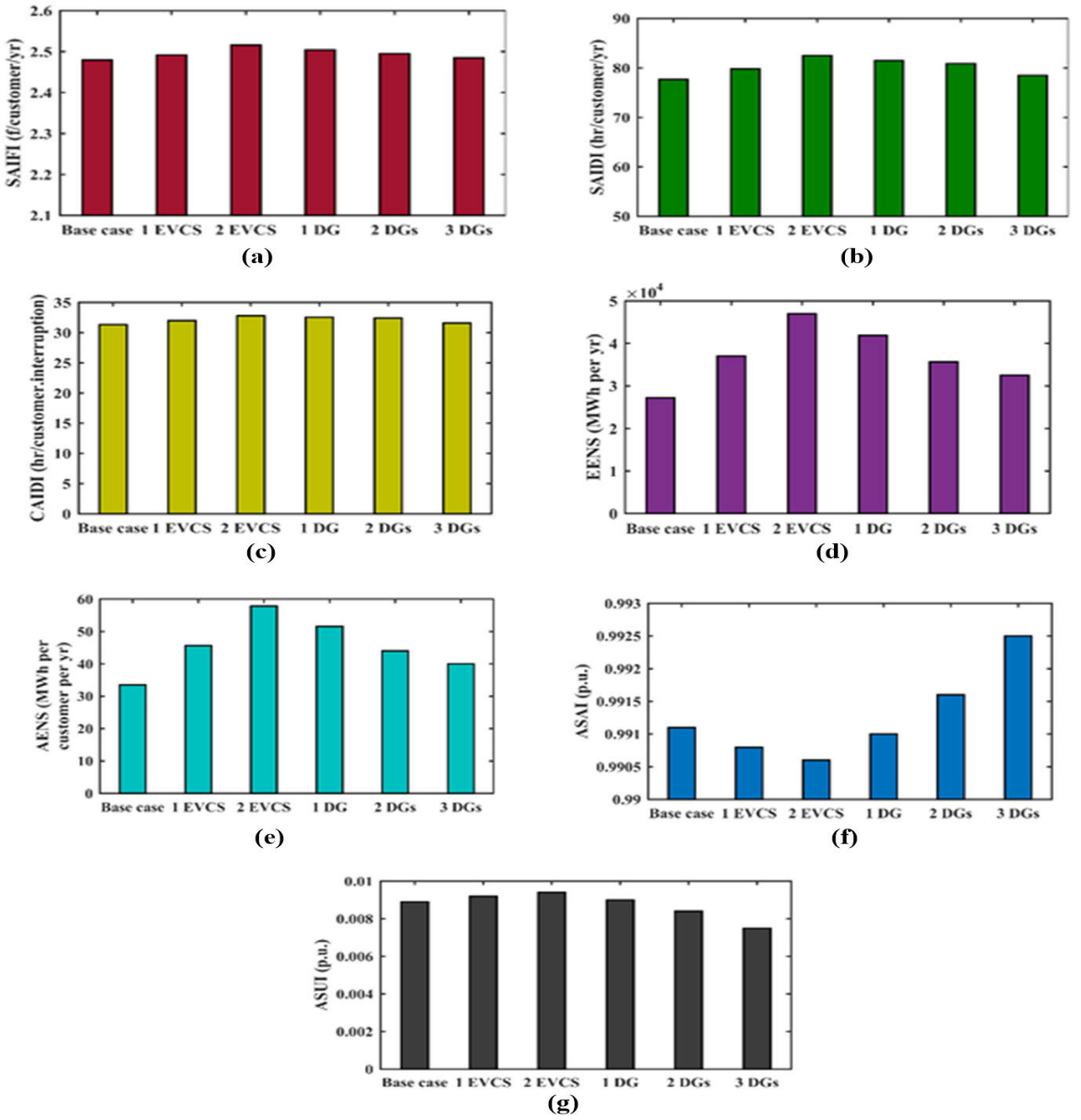

FIGURE 17. Variation in reliability indices with integration of EVCS and DGs in 69-bus system.

interruption respectively. Hence, these reliability indices continue to reduce with the increasing integration of DGs. As more DGs are introduced into the network, the period of the disturbance and the number of interruptions that occur in the system decrease. Therefore, the SAIDI and SAIFI have been decreased. Furthermore, a reduction in SAIDI and SAIFI values is desired for improving the reliability of the distribution system.

It's worth noting that the EENS and AENS reduce as the number of DGs increases. The value of AENS is 9.5381 MWh per customer per year with one DG only, whereas it is reduced to 7.0946 MWh per customer per year when one more DG is added into the system. As more DGs are incorporated into the network, the supplied energy to the system improves, and the indices for energy not supplied decrease. The reduction in EENS and AENS values is desirable for a reliable

power system. Hence, the reliability of the electrical system improves with the integration of DGs with adequate reliability data.

Also, DGs integration has positive impacts on electrical supply-based reliability indices, i.e., ASAI and ASUI. It is noted from Table 11. ASAI values increase with increasing DGs integration. The increase in ASAI results in a decrease in ASUI, which is beneficial for improving system reliability. Fig. 16. shows the impact of EV charging loads and DG units on various reliability indices in the 33-bus network.

2) RELIABILITY ANALYSIS FOR 69-BUS SYSTEM

This section of the article provides the impact on the reliability of the 69-bus distribution system after the optimal integration of EV charging loads followed by DG units. Here, 2 EVCS and 3 DGs are placed, which is different from the case of the 33-bus system where only two DGs were integrated. Table 12 and Table 13 report the statistical parameters such as failure rate, repair rate and average outage time, and customer information for the 69-bus system, respectively.

Similar to the 33-bus system, the addition of charging loads disturbs the customer as well as load-oriented reliability indices of the 69-bus system. DGs are integrated to maintain the reliability of the power system network by injecting energy to the system, thereby resulting in power loss reduction. The effect of integrating EV charging loads and DG units on various reliability indices in the 69-bus system is illustrated in Table 14.

As explained in the case of 33-bus system, the value of all customer-oriented reliability indices, i.e., SAIFI, SAIDI, and CAIDI increases from the base value after the integration of EV charging loads which are not desirable for a reliable power system. Similarly, load-oriented indices, i.e., EENS and AENS, also degrades due to the addition of EVCS. The value of all indices increases from their respective base value when charging loads are integrated. Hence, DGs are integrated as in case of 33- bus network to bring the system to operate in reliable mode. With the increasing integration of DGs, all the reliability indices improve, i.e., SAIFI, SAIDI, CAIDI, EENS, and AENS reduce, which is required from the reliability point of view of the distribution system.

Additionally, ASAI decreases when EVCS is placed. On the other hand, it goes on the increase with the integration of DGs, which is desirable. Fig. 17. shows the impact of EV charging loads and DG units on various reliability indices in the 69-bus network.

VI. CONCLUSION

Electric vehicles are a viable option for reducing transportation-related pollution. The rising reputation of EVs has resulted in the setting up of EVCSs; though, the negative influence of EV charging station loads on the electrical system cannot be overlooked. This paper presents the EVCS impact on the IEEE standard system based on a direct approach-based load flow analysis. The process of charging electric vehicles necessitates additional power from the grid, resulting in greater power losses. As a result, DG should be employed to offset the power losses generated by EVCS. Type 2 DG is utilized in this work, which repays for the system's power loss. Furthermore, a hybrid algorithm called HGWOPSO has been employed to reduce losses by determining the optimal node for EVCS and DG placement.

The proposed hybrid algorithm is validated on the IEEE-33 and IEEE-69 bus systems. Additionally, the accuracy of the suggested method is validated by comparing the outcomes acquired using other methodological approaches such as GWO and PSO. It is observed that HGWOPSO shows a significant reduction in system losses when compared to GWO and PSO for 33-bus as well as 69-bus systems.

Apart from the voltage and current constraints, the number of EV charging loads are fixed, and DGs are added into the grid network to reduce the system's losses. It is easy for the power engineers to choose the number of DGs for compensating the influence of EVCS by analyzing the mismatch in the capacity of the additional EVCS load and total system load. In the IEEE-33 bus system, two DGs satisfactorily improve the performance of the system, whereas the quantity of DGs required in the IEEE-69 bus system is four. Although power losses are minimized, and the voltage profile gets enhanced on increasing the DGs, the impact of specific fourth DG is marginal.

In addition, reliability analysis is performed to determine the cumulative influence of EV loads and DGs on the distribution system's health. All reliability indices are investigated in different scenarios. It is noticed that the placement of EVCS degrades the reliability of the network in 33-bus and 69-bus systems. However, results show that the DGs incorporation along with EVCS improves the reliability indices.

However, the current research work has several limitations, such as the use of a stochastic approach to construct the EV load at charging stations in order to estimate the impact of increased EV demand on the distribution system. Furthermore, rather than conventional DGs, renewable-based DGs, such as solar/wind, may be included. Additionally, coupled transportation and distribution networks can be taken as a test system.

Following are the research problems that can be addressed in the future:

- By taking into account larger standard IEEE systems like the 118-bus.
- Subsystem reliability data can also be added, providing a precise picture of the total system's reliability.
- The number of branches in a power system can also be changed to improve reliability, which is referred to as system reconfiguration. Furthermore, the dependency on CO2 emissions, as well as the protection and security of power system components, can also be addressed when assessing the system's reliability.
- A more systematic approach to charging station location issues could be investigated, taking into account EV consumers' activity-based behavior.
- Variations in daytime load, fluctuations in environmental variables such as temperature, irradiance, and

the wind, which might affect DGs such as solar photovoltaic and wind turbines, should be considered appropriately.

ACKNOWLEDGMENT

The authors would like to thank the Chair of Prince Faisal for Artificial intelligence research (CPFAI) for funding this research work through the project number QU-CPFAI-2-9-5. Also would like to extend their appreciation to the Deputyship for Research & Innovation, Ministry of Education and the Deanship of Scientific Research, Qassim University for their support for this research.

REFERENCES

[1] Z. Liu, F. Wen, and G. Ledwich, "Optimal planning of electric-vehicle charging stations in distribution systems," *IEEE Trans. Power Del.*, vol. 28, no. 1, pp. 102–110, Jan. 2013, doi: 10.1109/TPWRD.2012.2223489.

[2] H. R. Galiveeti, A. K. Goswami, and N. B. Dev Choudhury, "Impact of plug-in electric vehicles and distributed generation on reliability of distribution systems," *Eng. Sci. Technol., Int. J.*, vol. 21, no. 1, pp. 50–59, Feb. 2018, doi: 10.1016/j.jestch.2018.01.005.

[3] H. Mehrjerdi and E. Rakhshani, "Vehicle-to-grid technology for cost reduction and uncertainty management integrated with solar power," *J. Cleaner Prod.*, vol. 229, pp. 463–469, Aug. 2019, doi: 10.1016/j.jclepro.2019.05.023.

[4] M. Tomasov, D. Motyka, M. Kajanova, and P. Bracinik, "Modelling effects of the distributed generation supporting e-mobility on the operation of the distribution power network," *Transp. Res. Proc.*, vol. 40, pp. 556–563, Jan. 2019, doi: 10.1016/j.trpro.2019.07.080.

[5] W. Kempton and J. Tomić, "Vehicle-to-grid power implementation: From stabilizing the grid to supporting large-scale renewable energy," *J. Power Sources*, vol. 144, no. 1, pp. 280–294, 2005, doi: 10.1016/j.jpowsour.2004.12.022.

[6] D. C. Crowley, "Comparative environmental analysis of both plug-in hybrid and battery electric cars in Azerbaijan," Maastricht Univ., Maastricht, The Netherlands, Tech. Rep., 2020, doi: 10.13140/RG.2.2.34695.55207.

[7] S. Faddel, A. Al-Awami, and O. Mohammed, "Charge control and operation of electric vehicles in power grids: A review," *Energies*, vol. 11, no. 4, p. 701, Mar. 2018, doi: 10.3390/en11040701.

[8] Z. Darabi and M. Ferdowsi, "Aggregated impact of plug-in hybrid electric vehicles on electricity demand profile," *IEEE Trans. Sustain. Energy*, vol. 2, no. 4, pp. 501–508, Oct. 2011, doi: 10.1109/TSTE.2011.2158123.

[9] S. Shafiee, M. Fotuhi-Firuzabad, and M. Rastegar, "Investigating the impacts of plug-in hybrid electric vehicles on power distribution systems," *IEEE Trans. Smart Grid*, vol. 4, no. 3, pp. 1351–1360, Sep. 2013, doi: 10.1109/TSG.2013.2251483.

[10] M. K. Gray and W. G. Morsi, "On the impact of single-phase plug-in electric vehicles charging and rooftop solar photovoltaic on distribution transformer aging," *Electr. Power Syst. Res.*, vol. 148, pp. 202–209, Jul. 2017, doi: 10.1016/j.epsr.2017.03.022.

[11] P. Papadopoulos, S. Skarvelis-Kazakos, I. Grau, L. M. Cipcigan, and N. Jenkins, "Electric vehicles' impact on British distribution networks," *IET Electr. Syst. Transp.*, vol. 2, no. 3, p. 91, Oct. 2012, doi: 10.1049/iet-est.2011.0023.

[12] M. Etezadi-Amoli, K. Choma, and J. Stefani, "Rapid-charge electric-vehicle stations," *IEEE Trans. Power Del.*, vol. 25, no. 3, pp. 1883–1887, Jul. 2010, doi: 10.1109/TPWRD.2010.2047874.

[13] M. Bilal and M. Rizwan, "Electric vehicles in a smart grid: A comprehensive survey on optimal location of charging station," *IET Smart Grid*, vol. 3, no. 3, pp. 267–279, Jun. 2020, doi: 10.1049/iet-stg.2019.0220.

[14] S. Deb, K. Tammi, K. Kalita, and P. Mahanta, "Impact of electric vehicle charging station load on distribution network," *Energies*, vol. 11, no. 1, p. 178, 2018, doi: 10.3390/en11010178.

[15] C. H. Dharmakeerthi and N. Mithulananthan, "PEV load and its impact on static voltage stability," School Inf. Technol. Elect. Eng., Univ. Queensland, Brisbane, QLD, Australia, Tech. Rep., 2015, pp. 221–248, doi: 10.1007/978-981-287-299-9_8.

[16] A. Pal, A. Bhattacharya, and A. K. Chakraborty, "Allocation of EV fast charging station with V2G facility in distribution network," in *Proc. 8th Int. Conf. Power Syst. (ICPS)*, Dec. 2019, pp. 1–6, doi: 10.1109/ICPS48983.2019.9067574.

[17] A. Pal, A. Bhattacharya, and A. K. Chakraborty, "Allocation of electric vehicle charging station considering uncertainties," *Sustain. Energy, Grids Netw.*, vol. 25, Mar. 2021, Art. no. 100422, doi: 10.1016/j.segan.2020.100422.

[18] Y. Zhang, Q. Zhang, A. Farnoosh, S. Chen, and Y. Li, "GIS-based multi-objective particle swarm optimization of charging stations for electric vehicles," *Energy*, vol. 169, pp. 844–853, Feb. 2019, doi: 10.1016/j.energy.2018.12.062.

[19] S. Deb, K. Tammi, K. Kalita, and P. Mahanta, "Charging station placement for electric vehicles: A case study of Guwahati city, India," *IEEE Access*, vol. 7, pp. 100270–100282, 2019, doi: 10.1109/ACCESS.2019.2931055.

[20] F. Ahmad, M. Khalid, and B. K. Panigrahi, "An enhanced approach to optimally place the solar powered electric vehicle charging station in distribution network," *J. Energy Storage*, vol. 42, Oct. 2021, Art. no. 103090, doi: 10.1016/j.est.2021.103090.

[21] K. Qian, C. Zhou, M. Allan, and Y. Yuan, "Modeling of load demand due to EV battery charging in distribution systems," *IEEE Trans. Power Syst.*, vol. 26, no. 2, pp. 802–810, May 2011, doi: 10.1109/TPWRS.2010.2057456.

[22] L. P. Fernández, T. G. S. Román, R. Cossent, C. M. Domingo, and P. Frías, "Assessment of the impact of plug-in electric vehicles on distribution networks," *IEEE Trans. Power Syst.*, vol. 26, no. 1, pp. 206–213, Feb. 2011, doi: 10.1109/TPWRS.2010.2049133.

[23] X. Wang and R. Karki, "Exploiting PHEV to augment power system reliability," *IEEE Trans. Smart Grid*, vol. 8, no. 5, pp. 2100–2108, Sep. 2017, doi: 10.1109/TSG.2016.2515989.

[24] D. Božic and M. Pantoš, "Impact of electric-drive vehicles on power system reliability," *Energy*, vol. 83, pp. 511–520, Apr. 2015, doi: 10.1016/j.energy.2015.02.055.

[25] S. Deilami, A. S. Masoum, P. S. Moses, and M. A. S. Masoum, "Real-time coordination of plug-in electric vehicle charging in smart grids to minimize power losses and improve voltage profile," *IEEE Trans. Smart Grid*, vol. 2, no. 3, pp. 456–467, Sep. 2011, doi: 10.1109/TSG.2011.2159816.

[26] J. Y. Yong, V. K. Ramachandaramurthy, K. M. Tan, and N. Mithulananthan, "Bi-directional electric vehicle fast charging station with novel reactive power compensation for voltage regulation," *Int. J. Elect. Power Energy Syst.*, vol. 64, pp. 300–310, Jan. 2015, doi: 10.1016/j.ijepes.2014.07.025.

[27] M. Dixit, P. Kundu, and H. R. Jariwala, "Incorporation of distributed generation and shunt capacitor in radial distribution system for techno-economic benefits," *Eng. Sci. Technol., Int. J.*, vol. 20, no. 2, pp. 482–493, Apr. 2017, doi: 10.1016/j.jestch.2017.01.003.

[28] M. F. Shaaban, Y. M. Atwa, and E. F. El-Saadany, "PEVs modeling and impacts mitigation in distribution networks," *IEEE Trans. Power Syst.*, vol. 28, no. 2, pp. 1122–1131, May 2013, doi: 10.1109/TPWRS.2012.2212467.

[29] M. S. K. Reddy and K. Selvajyothi, "Optimal placement of electric vehicle charging station for unbalanced radial distribution systems," *Energy Sour., A, Recovery, Utilization, Environ. Effects*, vol. 2020, pp. 1–15, Feb. 2020, doi: 10.1080/15567036.2020.1731017.

[30] R. Sanjay, T. Jayabarathi, T. Raghunathan, V. Ramesh, and N. Mithulananthan, "Optimal allocation of distributed generation using hybrid Grey Wolf optimizer," *IEEE Access*, vol. 5, pp. 14807–14818, 2017, doi: 10.1109/ACCESS.2017.2726586.

[31] L. Liu, Y. Zhang, C. Da, Z. Huang, and M. Wang, "Optimal allocation of distributed generation and electric vehicle charging stations based on intelligent algorithm and bi-evel programming," *Int. Trans. Electr. Energy Syst.*, vol. 30, no. 6, pp. 1–21, Jun. 2020, doi: 10.1002/2050-7038.12366.

[32] D. Singh, D. Singh, and K. S. Verma, "GA based energy loss minimization approach for optimal sizing & placement of distributed generation," *Int. J. Knowl.-Based Intell. Eng. Syst.*, vol. 12, no. 2, pp. 147–156, May 2008, doi: 10.3233/KES-2008-12206.

[33] A. Ameli, S. Bahrami, F. Khazaeli, and M.-R. Haghifam, "A multiobjective particle swarm optimization for sizing and placement of DGs from DG owner's and distribution company's viewpoints," *IEEE Trans. Power Del.*, vol. 29, no. 4, pp. 1831–1840, Aug. 2014, doi: 10.1109/TPWRD.2014.2300845.

[34] M. H. Moradi and M. Abedini, "A combination of genetic algorithm and particle swarm optimization for optimal DG location and sizing in distribution systems," *Int. J. Elect. Power Energy Syst.*, vol. 34, no. 1, pp. 66–74, Jan. 2012, doi: 10.1016/j.ijepes.2011.08.023.

[35] M. A. Tolba, H. Rezk, M. Al-Dhaifallah, and A. A. Eisa, "Heuristic optimization techniques for connecting renewable distributed generators on distribution grids," *Neural Comput. Appl.*, vol. 32, no. 17, pp. 14195–14225, Sep. 2020, doi: 10.1007/s00521-020-04812-y.

[36] O. Erdinç, A. Tascikaraovğlu, N. G. Paterakis, İ. Dursun, M. C. Sinim, and J. P. S. Catalao, "Comprehensive optimization model for sizing and siting of DG units, EV charging stations, and energy storage systems," *IEEE Trans. Smart Grid*, vol. 9, no. 4, pp. 3871–3882, Jul. 2018, doi: 10.1109/TSG.2017.2777738.
[37] A. Selim, S. Kamel, A. S. Alghamdi, and F. Jurado, "Optimal placement of DGs in distribution system using an improved Harris hawks optimizer based on single- and multi-objective approaches," *IEEE Access*, vol. 8, pp. 52815–52829, 2020, doi: 10.1109/ACCESS.2020.2980245.
[38] K. B. Babu and S. Maheswarapu, "A solution to multi-objective optimal accommodation of distributed generation problem of power distribution networks: An analytical approach," *Int. Trans. Electr. Energy Syst.*, vol. 29, no. 10, pp. 1–20, Oct. 2019, doi: 10.1002/2050-7038.12093.
[39] K. Hesaroor and D. Das, "Annual energy loss reduction of distribution network through reconfiguration and renewable energy sources," *Int. Trans. Electr. Energy Syst.*, vol. 29, no. 11, pp. 1–21, Nov. 2019, doi: 10.1002/2050-7038.12099.
[40] M. BiazarGhadikolaei, M. Shahabi, and T. Barforoushi, "Expansion planning of energy storages in microgrid under uncertainties and demand response," *Int. Trans. Electr. Energy Syst.*, vol. 29, no. 11, pp. 1–20, Nov. 2019, doi: 10.1002/2050-7038.12110.
[41] M. Bilal and M. Rizwan, "Integration of electric vehicle charging stations and capacitors in distribution systems with vehicle-to-grid facility," *Energy Sour., A, Recovery, Utilization, Environ. Effects*, vol. 2021, pp. 1–30, May 2021, doi: 10.1080/15567036.2021.1923870.
[42] E. Akhavan-Rezai, M. F. Shaaban, E. F. El-Saadany, and F. Karray, "Managing demand for plug-in electric vehicles in unbalanced LV systems with photovoltaics," *IEEE Trans. Ind. Informat.*, vol. 13, no. 3, pp. 1057–1067, Jun. 2017, doi: 10.1109/TII.2017.2675481.
[43] S. Pazouki, A. Mohsenzadeh, S. Ardalan, and M.-R. Haghifam, "Simultaneous planning of PEV charging stations and DGs considering financial, technical, and environmental effects," *Can. J. Electr. Comput. Eng.*, vol. 38, no. 3, pp. 238–245, 2015, doi: 10.1109/CJECE.2015.2436811.
[44] B. Zeng, J. Feng, J. Zhang, and Z. Liu, "An optimal integrated planning method for supporting growing penetration of electric vehicles in distribution systems," *Energy*, vol. 126, pp. 273–284, May 2017, doi: 10.1016/j.energy.2017.03.014.
[45] S. J. Gunter, K. K. Afridi, and D. J. Perreault, "Optimal design of grid-connected PEV charging systems with integrated distributed resources," *IEEE Trans. Smart Grid*, vol. 4, no. 2, pp. 956–967, Jun. 2013, doi: 10.1109/TSG.2012.2227514.
[46] S. F. Abdelsamad, W. G. Morsi, and T. S. Sidhu, "Impact of wind-based distributed generation on electric energy in distribution systems embedded with electric vehicles," *IEEE Trans. Sustain. Energy*, vol. 6, no. 1, pp. 79–87, Jan. 2015, doi: 10.1109/TSTE.2014.2356551.
[47] K. Nekooei, M. M. Farsangi, H. Nezamabadi-Pour, and K. Y. Lee, "An improved multi-objective harmony search for optimal placement of DGs in distribution systems," *IEEE Trans. Smart Grid*, vol. 4, no. 1, pp. 557–567, Mar. 2013, doi: 10.1109/TSG.2012.2237420.
[48] J.-H. Teng, "A direct approach for distribution system load flow solutions," *IEEE Trans. Power Del.*, vol. 18, no. 3, pp. 882–887, Jul. 2003, doi: 10.1109/TPWRD.2003.813818.
[49] D. P. Kothari, "Power system optimization," in *Proc. 2nd Nat. Conf. Comput. Intell. Signal Process. (CISP)*, Mar. 2012, pp. 18–21, doi: 10.1109/NCCISP.2012.6189669.
[50] S. Sultana and P. K. Roy, "Multi-objective quasi-oppositional teaching learning based optimization for optimal location of distributed generator in radial distribution systems," *Int. J. Elect. Power Energy Syst.*, vol. 63, pp. 534–545, Dec. 2014, doi: 10.1016/j.ijepes.2014.06.031.
[51] I. A. Quadri, S. Bhowmick, and D. Joshi, "A comprehensive technique for optimal allocation of distributed energy resources in radial distribution systems," *Appl. Energy*, vol. 211, pp. 1245–1260, Feb. 2018, doi: 10.1016/j.apenergy.2017.11.108.
[52] M. Rizwan, U. Nangia, and A. Kumar, "A new approach to design and optimize sizing of hybrid microgrid in deregulated electricity environment," *CSEE J. Power Energy Syst.*, vol. 2020, pp. 1–11, Dec. 2020, doi: 10.17775/CSEEJPES.2020.03200.
[53] N. Chopra, G. Kumar, and S. Mehta, "Hybrid GWO-PSO algorithm for solving convex economic load dispatch problem," *Int. J. Res. Adv. Technol.*, vol. 4, no. 6, pp. 37–41, 2016.
[54] H. M. Hasanien, "Particle swarm design optimization of transverse flux linear motor for weight reduction and improvement of thrust force," *IEEE Trans. Ind. Electron.*, vol. 58, no. 9, pp. 4048–4056, Sep. 2011, doi: 10.1109/TIE.2010.2100338.
[55] S. Mirjalili, S. M. Mirjalili, and A. Lewis, "Grey wolf optimizer," *Adv. Eng. Softw.*, vol. 69, pp. 46–61, Mar. 2014, doi: 10.1016/j.advengsoft.2013.12.007.
[56] A. A. El-Fergany and H. M. Hasanien, "Single and multi-objective optimal power flow using grey wolf optimizer and differential evolution algorithms," *Electr. Power Compon. Syst.*, vol. 43, no. 13, pp. 1548–1559, Aug. 2015, doi: 10.1080/15325008.2015.1041625.
[57] S. Kumar, K. Sarita, A. S. S. Vardhan, R. M. Elavarasan, R. K. Saket, and N. Das, "Reliability assessment of wind-solar PV integrated distribution system using electrical loss minimization technique," *Energies*, vol. 13, no. 21, p. 5631, Oct. 2020, doi: 10.3390/en13215631.
[58] D. Kumar, S. R. Samantaray, I. Kamwa, and N. C. Sahoo, "Reliability-constrained based optimal placement and sizing of multiple distributed generators in power distribution network using cat swarm optimization," *Electr. Power Compon. Syst.*, vol. 42, no. 2, pp. 149–164, Jan. 2014, doi: 10.1080/15325008.2013.853215.

MOHD BILAL received the B.Tech. degree in electrical engineering and the M.Tech. degree in instrumentation and control engineering from Aligarh Muslim University, Aligarh, India, in 2014 and 2016, respectively. He is currently pursuing the Ph.D. degree with Delhi Technological University, New Delhi, India. He has published/presented few technical papers and conference proceedings in international journal of repute. His research interests include electric vehicles and optimization techniques.

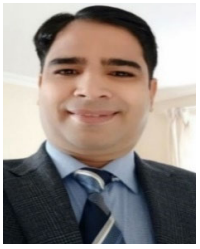

M. RIZWAN (Senior Member, IEEE) did his postdoctoral research at Virginia Polytechnic Institute and State University, USA. He is currently working as a Professor with the Department of Electrical Engineering, Delhi Technological University, Delhi, India. He has more than 19 years of teaching and research experience. He has successfully completed three research projects in the area of renewable energy systems and published and presented more than 155 research articles in reputed international/national journals, including IEEE TRANSACTIONS and conference proceedings. Recently, he has received a research project from Science and Engineering Research Board, DST, Government of India, in the area of energy management. He has published one book titled *Grid Integration of Solar Photovoltaic Systems*, CRC Press, (Taylor and Francis Group, 2017). He is currently editing one book for AIP Publishing, USA. He has written several book chapters also. His research interests include power system engineering, renewable energy systems particularly solar photovoltaic, building energy management, smart grid, and soft computing applications in renewable energy systems. He is a Life Member of ISTE and SSI and a member of International Association of Engineers (IAENG), and many other reputed societies. He was a recipient of Raman Fellowships for Postdoctoral Research for Indian Scholars, USA, from 2016 to 2017, and DST Start Up Grants (Young Scientists).

IBRAHIM ALSAIDAN (Member, IEEE) received the B.S. degree from Qassim University, Saudi Arabia, in 2008, and the M.S. and Ph.D. degrees from the University of Denver, in 2012 and 2018, respectively. He joined Qassim University, Buraydah, Saudi Arabia, in 2018, where he is currently an Assistant Professor with the Electrical Engineering Department. His current research interests include renewable energy and distributed generation, microgrid, smart grid, power system operation, and planning.

FAHAD M. ALMASOUDI (Member, IEEE) received the M.S. and Ph.D. degrees in electrical engineering from the University of Denver, USA, in 2013 and 2018, respectively. He is currently an Assistant Professor with the Department of Electrical Engineering, University of Tabuk, Tabuk, Saudi Arabia. His current research interests include renewable energy systems, dc–dc converters, inverters, modeling, and control of converters.